

Received: 17 August 2012 – Accepted: 20 August 2012 – Published: 14 September 2012

Correspondence to: K. G. Schulz (kschulz@geomar.de)

Published by Copernicus Publications on behalf of the European Geosciences Union.

BGD

9, 12543–12592, 2012

**Temporal biomass
dynamics of an Arctic
plankton bloom**

K. G. Schulz et al.

Title Page

Abstract

Introduction

Conclusions

References

Tables

Figures

◀

▶

◀

▶

Back

Close

Full Screen / Esc

Printer-friendly Version

Interactive Discussion



Abstract

Ocean acidification and carbonation, driven by anthropogenic emissions of carbon dioxide (CO₂), have been shown to affect a variety of marine organisms and are likely to change ecosystem functioning. High latitudes, especially the Arctic, will be the first to encounter profound changes in carbonate chemistry speciation at a large scale, namely the under-saturation of surface waters with respect to aragonite, a calcium carbonate polymorph produced by several organisms in this region. During a CO₂ perturbation study in 2010, in the framework of the EU-funded project EPOCA, the temporal dynamics of a plankton bloom was followed in nine mesocosms, manipulated for CO₂ levels ranging initially from about 185 to 1420 μatm. Dissolved inorganic nutrients were added halfway through the experiment. Autotrophic biomass, as identified by chlorophyll *a* standing stocks (Chl *a*), peaked three times in all mesocosms. However, while absolute Chl *a* concentrations were similar in all mesocosms during the first phase of the experiment, higher autotrophic biomass was measured at high in comparison to low CO₂ during the second phase, right after dissolved inorganic nutrient addition. This trend then reversed in the third phase. There were several statistically significant CO₂ effects on a variety of parameters measured in certain phases, such as nutrient utilization, standing stocks of particulate organic matter, and phytoplankton species composition. Interestingly, CO₂ effects developed slowly but steadily, becoming more and more statistically significant with time. The observed CO₂ related shifts in nutrient flow into different phytoplankton groups (mainly diatoms, dinoflagellates, prasinophytes and haptophytes) could have consequences for future organic matter flow to higher trophic levels and export production, with consequences for ecosystem productivity and atmospheric CO₂.

BGD

9, 12543–12592, 2012

Temporal biomass dynamics of an Arctic plankton bloom

K. G. Schulz et al.

Title Page

Abstract

Introduction

Conclusions

References

Tables

Figures

◀

▶

◀

▶

Back

Close

Full Screen / Esc

Printer-friendly Version

Interactive Discussion



1 Introduction

Anthropogenic emissions of carbon dioxide (CO₂) affect the oceans directly by shifting carbonate chemistry speciation, and indirectly by warming with associated changes in light and nutrient availability, potentially impacting autotrophic growth and biogeochemical element cycling (compare e.g. Sarmiento et al. (2004); Riebesell et al. (2009); Marinov et al. (2010) and references therein). Shifts in carbonate chemistry speciation include decreases in pH, carbonate ion concentrations and subsequently in carbonate saturation states (termed ocean acidification), and increases in bicarbonate and dissolved inorganic carbon concentrations (often referred to as ocean carbonation).

Ocean change is a global phenomenon, especially in surface waters, however, some regions are projected to be affected more, or more quickly, than others. High latitudes, with its cold seasurface temperatures have naturally low carbonate saturation states. Therefore, the Arctic is projected to be the first ocean region to become under-saturated on a larger scale for one of the calcium carbonate polymorphs, aragonite, already in a few decades (Steinacher et al., 2009). However, regionally and seasonally, Arctic sea ice melt or biological activity on top of ongoing ocean acidification can cause aragonite under-saturation already today (Bates et al., 2009; Yamamoto-Kawai et al., 2009). Also pH is projected to decrease more quickly, mainly due to melting ice and seawater freshening, but, this can be considered of minor importance in comparison to the overall changes (Steinacher et al., 2009).

At carbonate saturation states below One, i.e. under-saturation, calcium carbonate will start to dissolve. Aragonite and calcite, two forms of calcium carbonate, are produced by a variety of marine organisms such as foraminifera, coccolithophores, pteropods, corals, molluscs, echinoderms or coralline algae. Most of these have been shown to be impacted to a certain degree by ocean acidification in various laboratory studies, already at calcium carbonate over-saturated levels (see Kroeker et al., 2010 for a meta-analysis). How these organisms and associated communities will respond

BGD

9, 12543–12592, 2012

Temporal biomass dynamics of an Arctic plankton bloom

K. G. Schulz et al.

Title Page

Abstract

Introduction

Conclusions

References

Tables

Figures

◀

▶

◀

▶

Back

Close

Full Screen / Esc

Printer-friendly Version

Interactive Discussion



in their natural environment where species interaction and competition come into play, however, is largely unknown.

Mesocosm experiments, comprising natural plankton communities and several trophic levels, are an ideal platform for such research questions (compare Riebesell et al., 2008, 2012). Here we report on a mesocosm CO₂ perturbation study in the Arctic. One of the foci, the response of *Limacina helicina*, an important food-web component and marine calcium carbonate producing pteropod, to ongoing ocean acidification, had to be dropped, unfortunately, due to technical difficulties (see Sect. 2.1 for details). In the following we will describe the temporal biomass and phytoplankton assemblage dynamics during this experiment.

2 Methods

2.1 Mesocosm setup

On 31 May 2010 (day $t-7$), nine mesocosms were deployed at 78°56.2' N, 11° 53,6' E in the Kongsfjorden at Spitsbergen, the largest island of the archipelago of Svalbard (Norway). The floating structures of the **Kiel Off-Shore Mesocosms** for future **Ocean Simulations**, KOSMOS (compare Fig. 1), were moored in clusters of three, and filling of the attached cylindrical bags (0.5–1 mm thick, 17 m long and 2 m in diameter thermo-plastic polyurethane) started on the morning of the following day. For that purpose, the opened bottom plates of the bags were lowered carefully to 15 m depth, thereby slowly filling the mesocosms with natural fjord water. A 3 mm mesh-sized screen attached to the bottom plates excluded larger organisms such as pteropods which, due to their relatively patchy distribution in the water column, would not have been represented at equal abundances in all mesocosms. Furthermore, to minimize potential discrepancies in phytoplankton community composition between bags, caused by differences in timing of filling and small scale spatial separation of the mesocosms, the upper parts of the bags were pulled down about 1.5 m beneath the water surface. Again, a 3 mm

BGD

9, 12543–12592, 2012

Temporal biomass dynamics of an Arctic plankton bloom

K. G. Schulz et al.

Title Page

Abstract

Introduction

Conclusions

References

Tables

Figures

◀

▶

◀

▶

Back

Close

Full Screen / Esc

Printer-friendly Version

Interactive Discussion



mesh-sized screen attached to the upper part of the bags kept larger organisms outside the mesocosms which, now open to the fjord at both sides, integrated passing fjord water for about two days. Similarity between the seawater enclosed in each mesocosm was ensured by subsequent CTD casts, comparing vertical profiles of salinity, temperature, chlorophyll *a* (Chl *a*), turbidity, pH and oxygen concentrations. On the evening of 2 June the mesocosms were closed at the bottom by divers, while the upper parts of the bags were simultaneously retrieved and attached to the floating structures in about 2 m above the water surface. On top of the floating structures, about 0.5 m above the upper rim of the mesocosm bags, dome-shaped hoods minimized freshwater and dirt input from above. The closing of the bottom plates also unfolded a conical sediment trap in each mesocosm, about 2 m high and 2 m in diameter, thereby covering the entire bag (see also Riebesell et al., 2012).

Pteropods are important components of Arctic plankton communities. However, due to their patchy distribution they have been excluded during filling of the bags, avoiding otherwise uneven abundances between mesocosms. Adult pteropods of the species *Limacina helicina* were, therefore, hand-picked at different locations within the Kongsfjorden, and 100, 20 and 70 individuals were added to each mesocosm on days *t*4, 5 and 6, respectively. Unfortunately, they disappeared from the mesocosm water column relatively quickly. Most of them got trapped in the deadspace below the sediment traps (compare Fig. 1) and died, potentially related to their natural floating/sinking behavior.

2.2 Salt addition

Certain manipulations, such as dissolved inorganic nutrient addition, require knowledge of the exact seawater volume enclosed in each mesocosm bag. Otherwise, differences in volume would be directly reflected in nutrient concentration differences between mesocosms. The volume of each mesocosm was estimated by adding known amounts (50 kg per mesocosm) of sodium chloride (NaCl) enriched seawater (250 g NaCl per kg of seawater) and subsequent determination of changes in salinity (0.2 units). For that purpose, a dispersal device was lowered down to the opening of

BGD

9, 12543–12592, 2012

Temporal biomass dynamics of an Arctic plankton bloom

K. G. Schulz et al.

Title Page

Abstract

Introduction

Conclusions

References

Tables

Figures

◀

▶

◀

▶

Back

Close

Full Screen / Esc

Printer-friendly Version

Interactive Discussion



the conical sediment trap in 13 m depth and pulled up again to the surface for several times. Pumping of the NaCl enriched seawater through the dispersal device evenly distributed the salt addition in the mesocosm watercolumn. Vertical salinity profiles taken before and after were then used to determine the increase in salinity and hence estimate the seawater volume in each mesocosm bag, ranging between 43.9 and 47.6 m³. With the hand-operated memory probe CTD 60M from Sea and Sun Technology (see Sect. 2.5 for details) the typical uncertainty in volume estimate was found to be less than 1 %. For further details see Czerny et al. (2012b).

NaCl enriched seawater was added to each mesocosm twice, on day $t-4$ and $t4$ (compare Fig. 2). A second addition was found necessary as the volume estimate from the first was impaired by considerable uncertainties in initial salinity profiles. These uncertainties were caused by relatively slow (on the order of days) exchange and equilibration rates of the mesocosm water with that of the deadspace below the sediment trap (compare Fig. 1), which initially had a slightly higher salinity in comparison to average mesocosm water.

2.3 Carbon dioxide addition

1.5 m³ of 50 μ m filtered seawater taken from the fjord were aerated with pure CO₂ (99.995 %) for a minimum of 24 h. This CO₂ enriched seawater was used to increase dissolved inorganic carbon (DIC) and manipulate the carbonate system in seven out of nine mesocosms while the remaining two served as control. The addition was gradual between day $t-1$ and day $t4$ (compare Fig. 2) by pumping varying amounts of the CO₂ enriched seawater (compare Table 1) through a dispersal device which was lowered to about 13 m depth in the mesocosms and pulled up again for several times, resulting in an even distribution throughout the water column (compare Fig. 3). This way, a gradient of increasing partial pressures of carbon dioxide ($p\text{CO}_2$) and decreasing pH was created in the nine mesocosms, ranging after equilibration with the water in the deadspace between 185–1420 μ atm and 8.32–7.51, respectively (compare Table 1). Furthermore, the addition of CO₂ enriched seawater increased DIC while leaving total alkalinity (TA)

BGD

9, 12543–12592, 2012

Temporal biomass dynamics of an Arctic plankton bloom

K. G. Schulz et al.

Title Page

Abstract

Introduction

Conclusions

References

Tables

Figures

◀

▶

◀

▶

Back

Close

Full Screen / Esc

Printer-friendly Version

Interactive Discussion



constant, perfectly mimicking ongoing ocean acidification (compare Schulz et al., 2009; Gattuso, J.-P. and Lee, K. and Rost, B. and Schulz, K. G., 2010). For details on carbonate chemistry measurements and calculations see Bellerby et al. (2012).

2.4 Nutrient addition

5 A stock solution was prepared in 50 μm filtered fjord water, containing 10 mM nitrate, 0.62 mM phosphate and 5 mM silicate. For that, the respective sodium salts NaNO_3 , $\text{NaH}_2\text{PO}_4 \times \text{H}_2\text{O}$ and $\text{Na}_2\text{SiO}_3 \times 9 \text{H}_2\text{O}$ were solved in deionized water (18.2 M Ω) and added to the filtered seawater. Depending on mesocosm volume, 21.95–23.78 kg of this solution were then pumped into each mesocosm, employing the same technique
10 and dispersal device as for the CO_2 or NaCl enriched seawater additions (see above). The dissolved inorganic nutrient addition in the morning of day $t13$ (compare Fig. 2) was targeted to increase nitrate, phosphate and silicate concentrations by 5, 0.31 and $2.5 \mu\text{mol l}^{-1}$, respectively, and immediately followed by depth-integrated water sampling for nutrient analyzes. For the future it is recommended to prepare the nutrient stock
15 solution in deionized water as silicate at such relatively high concentrations was found to form precipitates in seawater, potentially in the form of sodium complexes. Although, these complexes slowly dissolve again when diluted in seawater, they interfere with biogenic silica measurements (see Sect. 3.5 for details).

2.5 Sampling procedures, CTD operation and light measurements

20 If not stated otherwise, depth integrated (0–12 m) samples were taken from each mesocosm and the fjord with an Integrating Water Sampler, IWS (HYDROBIOS), between 09:00 and 11:00 from boats. Except for gas samples, which were directly filled from the sampler into sampling bottles on board, water samples were brought back to shore and stored at in situ water temperature in the dark until further processing.

25 CTD casts were taken daily (except day $t22$) in each mesocosm and the fjord between 14:00 and 16:00 with a memory probe (CTD60M, Sea and Sun Technology).

Temporal biomass dynamics of an Arctic plankton bloom

K. G. Schulz et al.

Title Page

Abstract

Introduction

Conclusions

References

Tables

Figures

◀

▶

◀

▶

Back

Close

Full Screen / Esc

Printer-friendly Version

Interactive Discussion



The CTD was equipped with a conductivity cell, turbidity meter, fluorometer for chlorophyll *a*, and temperature, pH, dissolved oxygen and light sensors. For details on the sensors, respective accuracy and precision, and corrections applied, see Schulz and Riebesell (2012). Measured profiles, recorded with 5 data points per second and taken at 0.2–0.3 m s⁻¹, were scaled to a uniform depth resolution of 2 cm by linear interpolation.

Photosynthetic active radiation (PAR) was measured with two LICOR quantum sensors (LI-192) mounted onshore on top of a 1.5 m pole and on the roof of the French research station, “Charles Rabot”, at one measurement per second. In seawater PAR profiles were collected by means of a CTD mounted LICOR spherical quantum sensor (LI-193).

2.6 Analyzes

For particulate organic carbon and nitrogen (POC, PON), and total particulate carbon and nitrogen (TPC, TPN) analyzes, 400–500 ml of sample water were filtered (200 mbar) onto pre-combusted (450 °C for 5 h) GF/F filters, immediately stored frozen at –20 °C. Prior to analyzes filters were dried at 60 °C and subsequently measured on a EuroVector elemental analyzer according to Sharp (1974). POC filters were treated with fuming HCl in a desiccator for 2 h before drying and analysis. As there was no calcifying plankton found in microscopic counts, a mean of POC and TPC, and PON and TPN was calculated for each day and mesocosm.

For particulate organic phosphorus (POP) 400–500 ml of sample water were filtered onto pre-combusted (450 °C for 5 h) GF/F filters. POP was then oxidized to orthophosphate by heating the filters in 40 ml of deionized water (18.2 MΩ) with Oxisolv (MERCK) in a pressure cooker and determined colorimetrically on a Hitachi U2000 spectrophotometer (Hansen and Koroleff, 1999; Holmes et al., 1999).

For biogenic silica (BSi) 250–450 ml of sample water were filtered onto pre-combusted (450 °C for 5 h) GF/F filters. Alkaline, borate buffered persulphate oxidation in a pressure cooker was applied to transform biogenic BSi into silicate which was

Temporal biomass dynamics of an Arctic plankton bloom

K. G. Schulz et al.

Title Page

Abstract

Introduction

Conclusions

References

Tables

Figures



Back

Close

Full Screen / Esc

Printer-friendly Version

Interactive Discussion



subsequently determined spectrophotometrically (see Hansen and Koroleff (1999) for details).

Determination of dissolved organic nitrogen (DON) and phosphorus (DOP) was on GF/F (pre-combusted at 450 °C for 5 h) filtered sample water which was heated together with Oxisolv (MERCK) in a pressure cooker. Oxidized organic nitrogen and phosphorus was measured spectrophotometrically as nitrate (nitrite) and phosphate, respectively, on a Hitachi V2000 (Hansen and Koroleff, 1999; Holmes et al., 1999). DON and DOP was calculated from a simple mass-balance taking dissolved inorganic nutrient concentrations into account.

Dissolved inorganic carbon (DOC) was determined on GF/F (pre-combusted at 450 °C for 5 h) filtered sample water by high temperature catalytic oxidation (HTCO) on a SHIMADZU TOC-VCS. For details see Engel et al. (2012).

For chlorophyll *a* (Chl *a*) analysis 250–500 ml of sample water was filtered onto GF/F filters, immediately stored frozen for at least 24 h. Filters were then homogenized in 90 % acetone with glass beads (2 and 4 mm) in a cell mill. After centrifugation at 5000 rpm Chl *a* concentrations were determined in the supernatant on a fluorometer (TURNER, 10-AU) according to Welschmeyer (1994).

Preparations for pigment analyzes were like for Chl *a*, except that they were solved in 100 % acetone (HPLC grade), together with canthaxanthin as an internal standard to account for potential losses during sample handling. Pigment analyzes were by high performance liquid chromatography (WATERS HPLC with a VARIAN Microsorb-MV 100-3 C8 column) according to Barlow et al. (1997). Phytoplankton community composition was calculated with the CHEMTAX algorithm (Mackey et al., 1996), by converting the concentrations of marker pigments to Chl *a* equivalents with suitable pigment to Chl *a* ratios.

Dissolved inorganic nutrients nitrate (NO_3^-), nitrite (NO_2^-), ammonium (NH_4^+), phosphate (PO_4^{3-}) and silicate (H_4SiO_4) in the sample water were determined on a segmented flow analyzer (SEAL QuAatro) equipped with an autosampler. General methods described in Hansen and Koroleff (1999) were modified for nitrate (imidazole

BGD

9, 12543–12592, 2012

Temporal biomass dynamics of an Arctic plankton bloom

K. G. Schulz et al.

Title Page

Abstract

Introduction

Conclusions

References

Tables

Figures

◀

▶

◀

▶

Back

Close

Full Screen / Esc

Printer-friendly Version

Interactive Discussion



instead of an ammonium chloride buffer) and phosphate determinations, which followed Kerouel and Aminot (1997). SDS or Triton X-100 were used to lower surface tension and facilitate segmented flow analysis.

Counts of phytoplankton cells were on concentrated (25 ml) sample water, fixed with alkaline Lugol's iodine (1 % final concentration) in Utermöhl chambers with an inverted microscope (ZEISS Axiovert 100). At 200 times magnification cells larger than 12 μm were counted on half of the chamber area, while smaller ones were counted at 400 times magnification on two radial strips. Plankton was identified with the help of Tomas (1997); Hoppenrath et al. (2009); Kraberg et al. (2010) and von Quillfeldt (1996). Bio-volumes of counted plankton cells were calculated according to Olenina et al. (2006) and converted to cellular organic carbon quotas by the equations of Menden-Deuer and Lessard (2000).

2.7 Statistics

2.7.1 Linear regression analysis

Analyzes for potentially statistical significant correlations of various measurement parameters with seawater partial pressure of carbon dioxide ($p\text{CO}_2$) in each of the experimental phases (see below) were done by plotting the respective mean $p\text{CO}_2$ in each mesocosm during a certain phase against the mean of the measurement parameter to be tested. Linear regressions were analyzed with an F-test (see Table 2 for details).

2.7.2 Multivariate community analysis

First- and second-stage analyzes were applied to three sets of data, i.e. the organics (POC, PON, POP, DON and DOP), the CHEMTAX together with Chl *a*, and the phytoplankton carbon biomass dataset, to identify anomalous time trajectory profiles of the nine mesocosms resulting from conventional first-stage resemblance matrices (Clarke et al., 2006). When the time trajectories in the first-stage analysis of the treated

BGD

9, 12543–12592, 2012

Temporal biomass dynamics of an Arctic plankton bloom

K. G. Schulz et al.

Title Page

Abstract

Introduction

Conclusions

References

Tables

Figures

◀

▶

◀

▶

Back

Close

Full Screen / Esc

Printer-friendly Version

Interactive Discussion



mesocosms increasingly separate with increasing CO₂ and time from the control mesocosms, still plotting closely together, a CO₂ effect becomes visible. This can be identified in the second-stage analysis where the treated mesocosms should, depending on their CO₂ level, plot increasingly apart from the control mesocosms. To evaluate whether the time trajectories show any significant continuous pattern of change with increasing CO₂ level, a model severity matrix was created with a numeric factor for each mesocosm (0 for both controls and ascending from 1 to 7, in the order of CO₂ level, for the treated mesocosms). A subsequent RELATE test was run, comparing this model severity and second-stage matrix (Clarke and Gorley, 2006).

For the analyzes, the organics dataset was $\log(x + 1)$ transformed to remove some obvious skewness. The phytoplankton carbon biomass dataset was square root transformed prior to creating a resemblance matrix based on Bray-Curtis similarity (Clarke and Warwick, 2001). Additionally, the organics and the CHEMTAX + Chl *a* datasets were normalized prior to creating a resemblance matrix based on Euclidean distance. Furthermore, it was necessary to exclude measuring days with incomplete data of certain parameters, thus different numbers of days were included in the analyzes of the three datasets.

3 Results

3.1 Changes in light, salinity, temperature and oxygen concentrations

With the exception of a few days, measured incident photosynthetic active radiation (PAR) at ground level in air during polar night was not lower than 150 $\mu\text{mol m}^{-2} \text{s}^{-1}$. During polar day, maximum PAR levels were typically well above 700 and up to more than 1500 $\mu\text{mol m}^{-2} \text{s}^{-1}$ (compare Fig. 4). Vertical light profiles taken in all the mesocosms on each day showed little differences between mesocosms. Depending on bloom situation, 2–15% and 10–30% of PAR was measured at 14.5 m and 4.2 m depth, respectively in comparison to the surface layer between 0.01 to 0.02 m. Continuous light

BGD

9, 12543–12592, 2012

Temporal biomass dynamics of an Arctic plankton bloom

K. G. Schulz et al.

Title Page

Abstract

Introduction

Conclusions

References

Tables

Figures

◀

▶

◀

▶

Back

Close

Full Screen / Esc

Printer-friendly Version

Interactive Discussion



measurements for 40 h on days $t28$ to $t30$ in mesocosm M1 confirmed the light attenuation tendency by showing that, probably depending on cloud cover and solar elevation angle, four to six times less PAR was measured at 4.2 m depth in comparison to air during Polar day and night (data not shown).

In the fjord, depth-averaged (0.3–12 m) salinity varied between 32.94 and 34.03, with down to 29.59 at the surface and up to 34.29 at depth (compare Fig. 5a). In the mesocosms salinity was relatively stable, apart from the two salt additions on day $t-4$ and $t4$, and steadily increased by about 0.002 units per day (compare Fig. 5b), translating into a concentration change of all constituents of about 2‰ within the experimental period of about 30 days. As there was no significant precipitation, this phenomenon was driven by evaporation.

Temperatures in the mesocosms closely followed those in the fjord and started at about 2 °C, evenly distributed throughout the water column. Then water masses slowly warmed, especially in the upper 5 to 10 m, reaching depth-averaged (0.3–12 m) values of up to 5 °C until the end of the experiment (compare Fig. 5c).

Initial oxygen concentrations (depth-averaged) in the fjord and mesocosms was about 450 $\mu\text{mol kg}^{-1}$. Considering an oxygen solubility of 310 to 340 $\mu\text{mol kg}^{-1}$ at 2 to 5 °C at given salinities, waters were highly over-saturated. However, within a period of about 10 days, oxygen in the mesocosms decreased to saturation levels, probably driven by air/sea gas exchange. While concentrations remained close to these levels in the upper meters of the mesocosms, depth averaged (0.3–12 m) they steadily increased towards the end of the experiment by about 30 $\mu\text{mol kg}^{-1}$ (compare Fig. 5d).

3.2 Changes in pH

Initial pH levels in the fjord and mesocosms were relatively homogeneously distributed with depth at about 8.36 (reported on the total scale) as measured with a hand-operated CTD (Fig. 3). Additions of varying amounts of CO₂ enriched seawater (compare Table 1) to seven out of the nine mesocosms between day $t-1$ and day $t4$ decreased depth-averaged (0.3–12 m) pH to about 8.21, 8.04, 7.93, 7.82, 7.72, 7.64 and

Temporal biomass dynamics of an Arctic plankton bloom

K. G. Schulz et al.

Title Page

Abstract

Introduction

Conclusions

References

Tables

Figures

◀

▶

◀

▶

Back

Close

Full Screen / Esc

Printer-friendly Version

Interactive Discussion



7.49 in mesocosms M2, M4, M8, M1, M6, M5 and M9, respectively until days $t7-8$. Note that the slight increase in pH measured on the days right after the last addition was caused by water exchange with non-treated water masses in the deadspace below the sediment traps. While pH was relatively stable throughout the experiment in the control mesocosms M3 and M7, pH increased in the other mesocosms, mostly driven by an interplay of air/sea gas exchange and biological consumption and production of CO_2 (for details see Silyakova et al., 2012). Vertical pH distribution in the water column was relatively homogeneous throughout the experiment, with only slightly higher levels at the surface in the mesocosms with higher CO_2 (compare Fig. 3).

In the fjord, pH levels were relatively constant with time, as in the two control mesocosms.

3.3 Temporal chlorophyll *a* dynamics

Depth-averaged (0.3–12 m) chlorophyll *a* concentrations inside the mesocosms and the fjord started at about $0.2 \mu\text{g l}^{-1}$ at day $t-3$ and steadily increased to about 1– $1.4 \mu\text{g l}^{-1}$ in the mesocosms until day $t6-8$ (Fig. 6a). After that peak, chlorophyll *a* levels declined again to almost starting concentrations at day $t13$. Dissolved inorganic nutrient addition on that day (see next Sect. for details) initiated a second phytoplankton bloom, with higher chlorophyll *a* levels of up to $2 \mu\text{g l}^{-1}$ in the highest CO_2 treatment in comparison to about $1 \mu\text{g l}^{-1}$ in one of the control mesocosms on day $t19$. After the collapse of the second bloom, a third developed, but this time building up higher chlorophyll *a* concentrations in the mesocosms with lower in comparison to higher CO_2 levels.

Based on the temporal development of chlorophyll *a* dynamics four distinct phases were defined, i.e. phase 0 (from the start of the experiment to the end of the CO_2 addition, $t-4$ to $t4$), phase I (from the end of CO_2 enrichment to the end of the first bloom, $t4$ to $t13$), phase II (from the end of the first bloom to the end of the second bloom, $t13$ to $t22$) and phase III (from the end of the second bloom to the end of the experiment, $t22$ to $t30$). Chlorophyll *a* concentrations showed a statistically significant

12556

BGD

9, 12543–12592, 2012

Temporal biomass dynamics of an Arctic plankton bloom

K. G. Schulz et al.

Title Page

Abstract

Introduction

Conclusions

References

Tables

Figures

◀

▶

◀

▶

Back

Close

Full Screen / Esc

Printer-friendly Version

Interactive Discussion



linear correlation with CO₂ levels in phase II, while it was negative during phase III (compare Fig. 6a and Table 2).

In the fjord, temporal chlorophyll *a* dynamics were initially similar to those in the mesocosms, although reaching higher levels and peaking a few days later (compare Fig. 6a). Interestingly, there were signs of a second and the beginning of a third bloom phase in the fjord with similar timing as in the mesocosms, however, at lower intensities.

3.4 Dissolved inorganic nutrient dynamics with time

Initial nitrate (NO₃⁻) concentrations in the mesocosms were close to detection limit (about 0.1 μmol l⁻¹) and remained that low until the addition of dissolved inorganic nutrients on day *t*13. Initial ammonium (NH₄⁺) and phosphate (PO₄³⁻) concentrations in the mesocosms were measured at about 0.5–0.7 μmol l⁻¹ and 0.06–0.09 μmol l⁻¹, respectively. While ammonium relatively steadily decreased from then on, most of the phosphate initially present was taken up in the first couple of days (compare Fig. 6b, c, and d).

Additions of dissolved inorganic nutrients on day *t*13 increased NO₃⁻ and PO₄³⁻ concentrations to about 5.5 and 0.4 μmol l⁻¹, respectively. NO₃⁻ and PO₄³⁻ were then readily taken up by the plankton community, declining towards detection limits until the end of the experiment. Immediately after nutrient addition, however, nutrient utilization of both NO₃⁻ and PO₄³⁻ was faster at higher CO₂ levels during phase II, while being slower during phase III (Fig. 6b and d). This observation was statistically significant. NH₄⁺ concentrations were also correlated to CO₂ level in a statistically significant manner, negatively in phase II and positively in phase III of the experiment (compare Fig. 6c and Table 2).

Dynamics of NO₃⁻, PO₄³⁻ and NH₄⁺ in the fjord during phase 0 and I of the experiment were similar to those in the mesocosms. However, they remained at relatively low levels also in phase II and III (compare Fig. 6c).

BGD

9, 12543–12592, 2012

Temporal biomass dynamics of an Arctic plankton bloom

K. G. Schulz et al.

Title Page

Abstract

Introduction

Conclusions

References

Tables

Figures

◀

▶

◀

▶

Back

Close

Full Screen / Esc

Printer-friendly Version

Interactive Discussion



3.5 Silicate addition and silicon budget

Prior to the addition of dissolved inorganic nutrients on day $t13$ silicate concentrations, together with those of biogenic silica and total silicate (the sum of silicate and biogenic silica) were relatively stable in all mesocosms. However, during phase I there was a statistically significant correlation of silicate and total silicate with CO_2 , with higher concentrations towards lower CO_2 (compare Fig. 7a, c, and Table 2). The addition of silicate (targeted for about $2.5 \mu\text{mol l}^{-1}$) on day $t13$ to all mesocosms increased concentrations to only about $1.3\text{--}1.6 \mu\text{mol l}^{-1}$. The rest of the added silicate was in a precipitated form and increased biogenic silica concentrations to about $0.8\text{--}1.2 \mu\text{mol l}^{-1}$. In the first days after the nutrient addition, silicate continued to increase in all mesocosms, reaching higher concentrations at lower CO_2 levels, but then steadily declined towards the end of the experiment. While silica concentrations in phase II displayed a statistically significant negative correlation to CO_2 , those of biogenic silica were positively correlated (compare Fig. 7a, b, and Table 2). During that phase, also the amount of biogenic silica collected in the sediment traps was higher at higher CO_2 levels, although absolute amounts were relatively small compared to water column inventories (Fig. 7d). This trend reversed in phase III, when more biogenic silicate at lower CO_2 levels was collected in the sediment traps (again at relatively low concentrations), at a time when no CO_2 effect was observed on any of the water column silica components (Fig. 7).

3.6 Particulate and dissolved organic matter dynamics with time

Initial concentrations of particulate organic carbon (POC), nitrogen (PON) and phosphorus (POP) started at about $15\text{--}25 \mu\text{mol l}^{-1}$, $3\text{--}4 \mu\text{mol l}^{-1}$ and $0.2\text{--}0.3 \mu\text{mol l}^{-1}$, respectively (Fig. 8a, b and c). POC and PON peaked during phase I of the experiment, similar to chlorophyll a , however, this observation was less evident for POP. Both, POC and PON increased after nutrient addition in phase II and III, and again, this was less obvious for POP. During phase II, standing stocks of POC, PON and POP were positively correlated to CO_2 . This trend was statistically significant (compare Table 2).

BGD

9, 12543–12592, 2012

Temporal biomass dynamics of an Arctic plankton bloom

K. G. Schulz et al.

Title Page

Abstract

Introduction

Conclusions

References

Tables

Figures

◀

▶

◀

▶

Back

Close

Full Screen / Esc

Printer-friendly Version

Interactive Discussion



Temporal biomass dynamics of an Arctic plankton bloom

K. G. Schulz et al.

Title Page

Abstract

Introduction

Conclusions

References

Tables

Figures

◀

▶

◀

▶

Back

Close

Full Screen / Esc

Printer-friendly Version

Interactive Discussion



While temporal dynamics of POC, PON and POP were basically identical, those of dissolved organic carbon (DOC), nitrogen (DON) and phosphorus (DOP) were quite different. DOC, starting at about 70–80 $\mu\text{mol l}^{-1}$ in all mesocosms, increased before nutrient addition during phase 0 and I, resulting in higher concentrations at higher CO_2 in phase II. This positive correlation was statistically significant (compare Table 2). After nutrient addition, however, there seemed to be no further DOC accumulation (compare Fig. 8d). In contrast, DON, starting at about 5–6 $\mu\text{mol l}^{-1}$ in all mesocosms, steadily declined before nutrient addition during phase 0 and I by a bout 1 $\mu\text{mol l}^{-1}$, and remained rather constant from then on, although with considerable scatter in the data (Fig. 8e). Finally, DOP concentrations, starting at about 0.2 $\mu\text{mol l}^{-1}$ in all mesocosms, seemed rather constant during phase 0 and I, but increased after nutrient addition by 0.05–0.1 $\mu\text{mol l}^{-1}$ in all mesocosms during phase II, and then remained rather stable until the end of the experiment (Fig. 8f).

Dynamics of particulate and dissolved organic element concentrations in the fjord were similar to those in the mesocosms during phase 0 and I, with the exception of POC which peaked at higher concentrations (compare Fig. 8). However, after nutrient addition, absolute concentrations tended to be smaller.

3.7 Temporal dynamics of particulate and dissolved organic element stoichiometry

POC/PON started slightly below the classical Redfield stoichiometry (C/N/P of 106 : 16 : 1) in all mesocosms and increased during phase I (compare Fig. 9a). Nutrient addition at the beginning of phase II decreased POC/PON back below the Redfield ratio. However, during the end of phase III, POC/PON started to increase again, towards higher ratios at lower CO_2 . This trend in phase III was statistically significant (compare Table 2).

Both, POC/POP and PON/POP was close to the respective Redfield ratio during the entire experiment, although with considerable scatter in the data (compare Fig. 9b and c). Mesocosms with higher CO_2 had higher POC/POP and PON/POP in phase II,

an observation which was statistically significant (compare Table 2). During the last days of the experiment POC/POP started to increase in all mesocosms.

Both, DOC/DON and DON/DOP started (and remained) well above classical Redfield stoichiometry in all mesocosms (compare Fig. 9d and e). While DOC/DON steadily increased during phase 0 and I and remained rather constant during phase II and III, DOC/DOP relatively quickly increased towards the end of phase I and then declined throughout phase II, stabilizing again in phase III.

DON/DOP also started well above classical Redfield stoichiometry in all mesocosms, but then rather steadily declined throughout the experiment and stabilized towards the end slightly below its respective ratio (compare Fig. 9f).

Temporal dynamics of particulate and dissolved organic element stoichiometry in the fjord were similar to those in the mesocosms. An exception were absolute ratios of POC to PON, being higher during phase I and II (compare Fig. 9).

3.8 Temporal changes in phytoplankton community composition derived from HPLC analysis of marker pigments

Chl *a* as measured by HPLC followed the same temporal evolution, and most importantly with the same CO₂ related trends between treatments, as the fluorometric determinations, although at slightly lower absolute concentrations (compare Figs. 6a and 10).

According to CHEMTAX analysis, the Chl *a* peak during phase I was mostly due to the presence of haptophytes, with minor contributions of prasinophytes and diatoms (compare Fig. 10h, a and f, respectively). The second Chl *a* peak during phase II was dominated by the bloom of prasinophytes, dinoflagellates (especially at higher CO₂ levels) and cryptophytes (compare Fig. 10a, b and c, respectively). Finally, the third Chl *a* peak in phase III was driven by the growth of haptophytes, prasinophytes, dinoflagellates and chlorophytes, with the former being responsible for about half of autotrophic biomass (compare Fig. 10h, a, b and d, respectively). Cyanobacteria and chrysophytes contributed only marginally to the autotrophic biomass throughout the

BGD

9, 12543–12592, 2012

Temporal biomass dynamics of an Arctic plankton bloom

K. G. Schulz et al.

Title Page

Abstract

Introduction

Conclusions

References

Tables

Figures

◀

▶

◀

▶

Back

Close

Full Screen / Esc

Printer-friendly Version

Interactive Discussion



experiment (compare Fig. 10e and g). There were several statistically significant CO₂ effects on phytoplankton biomass, such as positive CO₂ correlations for prasinophytes, cryptophytes and chrysophytes (phase I and II), dinoflagellates (phase II and III) and haptophytes (phase II), and negative CO₂ correlations for prasinophytes and chlorophytes in phase III (compare Table 2).

Temporal phytoplankton dynamics as revealed by HPLC in the fjord was similar to the mesocosms for most groups, although at lower absolute biomass. An exception were prasinophytes and dinoflagellates, important contributors to autotrophic standing stocks in all mesocosms during phase II and III, having insignificant contributions in the fjord during this time (compare Fig. 10).

3.9 Temporal changes in plankton community composition as determined by light microscopy

As determined by microscopic counts, most autotrophic carbon biomass during phase I was found in chrysophytes and chlorophytes, although the latter could have been also *Phaeocystis*, belonging to the group of haptophytes (compare Fig. 11). During phase II most autotrophic carbon was found to be in dinoflagellates and again the chlorophytes (or haptophytes). Finally, phase III was clearly dominated by autotrophic dinoflagellates, with minor contributions by diatoms. As for HPLC derived phytoplankton community composition, there were statistically significant trends with CO₂, positive ones for autotrophic dinoflagellates, cryptophytes, chlorophytes (or haptophytes), chrysophytes and autotrophic flagellates other than dinoflagellates in phase II. During phase III carbon biomass by diatoms was higher at lower CO₂ levels, a trend found to be statistically significant (compare Table 2).

Compared to total autotrophic carbon, similar amounts (between 0.5 and 1.5 μmol l⁻¹) were found in heterotrophic flagellates (compare Fig. 11h). However, concentrations seemed to slightly decline during phase I in all mesocosms, while the dynamics during phase III appeared to be varying between mesocosms, although with no particular CO₂ trend.

BGD

9, 12543–12592, 2012

Temporal biomass dynamics of an Arctic plankton bloom

K. G. Schulz et al.

Title Page

Abstract

Introduction

Conclusions

References

Tables

Figures

◀

▶

◀

▶

Back

Close

Full Screen / Esc

Printer-friendly Version

Interactive Discussion



Dynamics of plankton carbon standing stocks in the fjord were similar to those in the mesocosms, but usually at lower absolute concentrations (compare Fig. 11). An exception were autotrophic dinoflagellates with insignificant and chrysophytes with higher carbon biomass in comparison to the mesocosms at certain times.

3.10 First- and second-stage analyses

First-stage MDS (multi-dimensional scaling) plots for the combined CHEMTAX and Chl *a* dataset showed no clear succession pattern between the control and the CO₂-treated mesocosms (Fig. 12a). Furthermore, the two control mesocosms (M3 and M7) had rather different patterns concerning their time trajectories, indicating natural variability of the enclosed plankton assemblages. Only the time trajectory of mesocosm M9 had a clear succession in the temporal evolution, in contrast to the others. Based on this, it is not clear whether there was a CO₂ effect on the temporal development of the phytoplankton community or whether it was masked by slightly different starting conditions. The second-stage MDS plot showed no clear separation between the control and treated mesocosms, probably related to differences between the controls. However, a differentiation according to CO₂ level is obvious. This was confirmed by the RELATE analysis, identifying the temporal pigment (CHEMTAX and Chl *a*) evolution, when the entire experiment was considered, to be statistically different and related to CO₂, at a significance level of 0.001 (compare Table 3).

First-stage MDS plots for the phytoplankton carbon biomass dataset showed a more consistent pattern among time trajectories of the control and treated mesocosms (Fig. 12b). In this respect, the two control mesocosms were considerably more similar as compared to those of the CHEMTAX and Chl *a* dataset and revealed also differences in their temporal evolution compared to the CO₂-treated mesocosms. For example, the days 14 and 16 plot far apart from each other in the control mesocosms M3 and M7, while the days 20 and 22 plot very close together. This was, with the exception of M5 and M9, not the case for the CO₂-treated mesocosms. As a result, the second-stage MDS plot, depicting similarity of the time trajectories among the mesocosms, clearly

Temporal biomass dynamics of an Arctic plankton bloom

K. G. Schulz et al.

Title Page

Abstract

Introduction

Conclusions

References

Tables

Figures



Back

Close

Full Screen / Esc

Printer-friendly Version

Interactive Discussion



separated the control from the CO₂-treated mesocosms. The REALTE analysis confirmed this observation, when the entire experiment was considered, identifying the temporal carbon biomass dynamics to be statistically different and related to CO₂, at a significance level of 0.048 (compare Table 3).

5 While the RELATE analysis, considering the entire experiment, identified the temporal development of phytoplankton pigments (CHEMTAX) and Chl *a*, and that of phytoplankton carbon biomass to be statistically different and related to CO₂, the dynamics in the organics dataset were not different at a statistically significant level (compare Table 3). Considering individual phases of the experiment, the temporal evolution of
10 phytoplankton pigments (CHEMTAX) and Chl *a*, was statistically different and related to CO₂ in phase III. Interestingly, while calculated levels of significance of the RELATE analyses were relatively high in the beginning of the experiment in phase I (thus not statistically significant), they steadily decreased throughout phase II and III.

4 Discussion and summary

15 4.1 Oceanographic setting

At the beginning of the experiment, the plankton community was clearly in a post-bloom phase, indicated by high O₂ and pH, and low *p*CO₂ levels in the water column. Oxygen levels were supersaturated by about 140 μmol kg⁻¹ in comparison to dissolved inorganic carbon (DIC), being under-saturated by about the same amount, when taking
20 initial measured mean total alkalinity (TA) and DIC and calculating DIC in atmospheric equilibrium using the dissociation constants for carbonic acid by Mehrbach et al. (1973) at in situ temperature and salinity (for details on carbonate chemistry see Bellerby et al., 2012). Considering that autotrophic growth, depending on nitrogen source, is typically producing 1–1.4 mol oxygen per mole DIC consumed (Laws, 1991), and that oxygen
25 exchanges with the atmosphere about ten times faster than carbon dioxide (Broecker

BGD

9, 12543–12592, 2012

Temporal biomass dynamics of an Arctic plankton bloom

K. G. Schulz et al.

Title Page

Abstract

Introduction

Conclusions

References

Tables

Figures

◀

▶

◀

▶

Back

Close

Full Screen / Esc

Printer-friendly Version

Interactive Discussion



and Peng, 1982), a phytoplankton bloom came to an end probably just a couple of days before the beginning of the experiment.

The relatively substantial amounts of ammonia in comparison to nitrate are indicative of a recycling system, typical for this location and time of the year (compare Iversen and Seuthe, 2011). The autotrophic community did not appear to be nutrient limited, as indicated by particulate organic carbon to nitrogen (POC/PON) below classical Redfield stoichiometry (Redfield et al., 1963), although most of the particulate organic matter was probably not in the autotrophic but rather heterotrophic compartment or detritus, as initial POC to Chl *a* ratios ($\mu\text{mol}/\mu\text{g}$) were well above 100. Typical ratios for phytoplankton range between 3 and 8 (Montagnes et al., 1994). Nevertheless, the increase in Chl *a* during phase 0 and I in all mesocosms is further indication that autotrophic biomass was initially not nutrient limited.

During the experimental period, considerable variability in salinity was measured in the fjord, being as low as 29.59 at the surface and up to 34.29 in 12 m depth. This was probably the result of changing relative influence of Arctic and Atlantic watermasses and meltwater runoff (compare Hop et al., 2006). Despite this watermass variability, general characteristics in plankton bloom development in the fjord were surprisingly similar to those in the mesocosms (see Sect. 4.6 for details).

4.2 Autotrophic biomass and nutrient dynamics

During phase 0 and then I, after CO_2 manipulation, a first phytoplankton bloom developed in all mesocosms, however, with no particular effect of CO_2 on actual concentrations of Chl *a* or particulate organic matter (compare Figs. 6a, and 8a, b and c). Taking the mean of all mesocosms, utilization of ~ 0.05 , ~ 0.2 and $\sim 0.7 \mu\text{mol l}^{-1}$ of phosphate, ammonium and DON, respectively, explain reasonably well the built-up of $\sim 9 \mu\text{mol l}^{-1}$ of POC during this time. Considering measurement uncertainties at such low nutrient concentrations and the relatively small POC production at much higher background levels, the bloom can be thought to have followed conventional Redfield proportions (Redfield et al., 1963), although carbon quotas seem elevated. The resulting POC to

Temporal biomass dynamics of an Arctic plankton bloom

K. G. Schulz et al.

Title Page

Abstract

Introduction

Conclusions

References

Tables

Figures



Back

Close

Full Screen / Esc

Printer-friendly Version

Interactive Discussion



Chl *a* ratio ($\mu\text{mol}/\mu\text{g}$) of ~ 9 (compare Figs. 6a and 8a) is about twice as high and at the upper range of reported values for marine phytoplankton (Montagnes et al., 1994). This indicates that a significant portion of the freshly produced autotrophic biomass was consumed by heterotrophic grazing, although not reflected by protozooplankton biomass during that time (Aberle et al., 2012). However, cirripedia nauplii, dominating the mesozooplankton community in this phase, grew to cypris larvae, the next developmental stage (Niehoff et al., 2012), and grazing by microzooplankton on nanoeukaryotes, an important phytoplankton component in this phase, probably haptophytes (compare Fig. 10h), was measured (Brussaard et al., 2012). Apart from grazing, viral lysis of phytoplankton was found to contribute to the termination of the first bloom (Brussaard et al., 2012).

4.2.1 Direct effects of CO₂ on marine phytoplankton

Interestingly, a positive effect of CO₂ on abundances of prasinophytes, probably identified by flowcytometry as picoeukaryotes (Brussaard et al., 2012), started to develop already in phase I. Nutrient addition on day *t*13 amplified this trend, and prasinophytes, dominating the phytoplankton community during phase II, clearly profited from higher CO₂ levels (also compare Brussaard et al., 2012). Associated dissolved inorganic nutrient drawdown of nitrate, phosphate and ammonium during the first part of phase II was also higher (compare Fig. 6b, c and d). This can fully be explained by higher autotrophic biomass built-up during this time. Assuming a mean carbon to Chl *a* ratio of 4 ($\mu\text{mol}/\mu\text{g}$) for autotrophic growth (Montagnes et al., 1994), would result in a nitrogen to Chl *a* ratio of about 0.6 ($\mu\text{mol}/\mu\text{g}$), meaning that for $1 \mu\text{g l}^{-1}$ of Chl *a* produced, $0.6 \mu\text{mol l}^{-1}$ of nitrate (or ammonium) is taken up. Differences in maximum Chl *a* levels and nutrient utilization between CO₂ treatments were on this exact order of magnitude (compare Fig. 6). Such direct effect of CO₂ on picoeukaryotes, most likely belonging to the group of prasinophytes, was also found in other mesocosm experiments where especially *Micromonas*-like (sic!) phylotypes profited from higher CO₂ levels (Paulino et al., 2008; Engel et al., 2008; Meakin and Wyman, 2011; Newbold et al., 2012). The

BGD

9, 12543–12592, 2012

Temporal biomass dynamics of an Arctic plankton bloom

K. G. Schulz et al.

Title Page

Abstract

Introduction

Conclusions

References

Tables

Figures

◀

▶

◀

▶

Back

Close

Full Screen / Esc

Printer-friendly Version

Interactive Discussion



reason for such pronounced CO₂ sensitivity could be speculated to be related to the mode of the cellular carbon concentrating mechanism (CCM) employed. *Micromonas* is known to operate a C-4 like carbon fixation pathway (Worden, 2009) and to express extra-cellular carbonic anhydrase (Iglesias-Rodríguez et al., 1998), facilitating the otherwise slow inter-conversion between carbon dioxide (CO₂) and bicarbonate (HCO₃⁻). However, its relatively small size (less than 2 µm in diameter) could make the extensive operation of active CO₂ and HCO₃⁻ uptake, like in most bigger phytoplankton species (compare e.g. Giordano et al. (2005) and references therein) unnecessary, as the diffusive boundary layer can be considered relatively small (Riebesell et al., 1993).

Also autotrophic dinoflagellates, as identified by microscopic counts and HPLC pigment analysis, profited from higher CO₂ during phase II (compare Fig. 11b). As they appear to possess only moderately efficient CCMs (see Reinfelder (2010) for a review and references therein), they also can be regarded potential winners in the phytoplankton community at increasing levels of carbon dioxide.

4.2.2 Indirect effects of CO₂ on marine phytoplankton

During phase III of the experiment, after termination of the second bloom by viral infection (see Brussaard et al. (2012) for details), the positive CO₂ effect on autotrophic biomass reversed (compare Fig. 6a). Now diatoms, prasinophytes and to a certain extent also haptophytes grew to higher abundances at low in comparison to high CO₂ (compare Figs. 10 and 11e). This is most likely an indirect CO₂ effect as after the collapse of the second bloom in phase II, more inorganic nutrients were available at lower CO₂ concentrations (compare Figs. 6b and d). This was at a time when dissolved silicate concentrations were similar in all mesocosms (compare Fig. 7). As the silicic frustules of diatoms are known to efficiently ballast organic matter, facilitating the export to depth (Armstrong et al., 2001; Francois et al., 2002; Klaas and Archer, 2002, but see also Passow, 2004), higher diatom-derived biomass could be connected to the higher organic biomass collected in the sediment traps in the mesocosms with lower CO₂ levels (see Czerny et al., 2012a for details). However, the experiment ended at a

Temporal biomass dynamics of an Arctic plankton bloom

K. G. Schulz et al.

Title Page

Abstract

Introduction

Conclusions

References

Tables

Figures



Back

Close

Full Screen / Esc

Printer-friendly Version

Interactive Discussion



time of relatively high sedimentation and it is thus not clear if the observation of more export at lower CO₂ would be a persistent signal. Nevertheless, global export production in the future and biomass transfer to higher trophic levels, could be affected if more nutrients are being utilized by small picoplankton, profiting from enhanced CO₂ levels, and rather being grazed by nano-/microzooplankton and remineralized in the surface ocean.

4.3 Comparison of phytoplankton biomass determination approaches

Although there are inherent uncertainties associated with converting phytoplankton counts to biovolume and relate this to organic matter standing stocks, according to microscopic counts, the carbon found in autotrophic biomass was relatively low in comparison to measured built-up of POC and Chl *a* (compare Figs. 11, 8, and 6a). Part of this seeming discrepancy could be connected to biomass transfer to higher trophic levels by grazing (compare Czerny et al., 2012a; Brussaard et al., 2012; Aberle et al., 2012 and Niehoff et al., 2012, but also Sect. 4.2). Furthermore, phytoplankton pigment analysis revealed prasinophytes (potentially *Micromonas*-like phylotypes) and haptophytes to dominate the autotrophic biomass during most of the experiment, an observation not picked up by light microscopy. This is probably related to their small size as *Micromonas* is less than 2 μm in diameter and most of the haptophyte carbon is usually found in the size-class below 3 μm, often dominating overall marine autotrophic biomass in the ocean (Lui et al., 2009; Uitz et al., 2010; Cuvelier, 2010). The dominance of picophytoplankton in certain phases of the experiment was confirmed by flowcytometry (see Brussaard et al. (2012) for details).

4.4 Temporal dynamics of particulate organic matter

Temporal dynamics, especially effects of CO₂, in and on standing stocks of particulate organic matter was not as clear as for Chl *a* and phytoplankton community composition (compare Figs. 8, 6a, 10 and 11). Given measurement uncertainties and relatively

BGD

9, 12543–12592, 2012

Temporal biomass dynamics of an Arctic plankton bloom

K. G. Schulz et al.

Title Page

Abstract

Introduction

Conclusions

References

Tables

Figures

◀

▶

◀

▶

Back

Close

Full Screen / Esc

Printer-friendly Version

Interactive Discussion



low autotrophic production on a relatively large particulate organic matter background, trends clearly seen in the autotrophic compartments only become visible in particulate organic matter dynamics when phytoplankton growth exceeds a certain threshold (also compare Kim et al., 2011), like after nutrient addition in phase II (compare Fig. 8a, b and c). Thus, the observation that there was no measurable effect of CO₂ on standing stocks of particulate organic matter such as carbon, observed in several mesocosm studies, does not allow the conclusion that autotrophic carbon built-up was not affected (compare Engel et al., 2005; Schulz et al., 2008). This also applies to stoichiometric ratios of particulate and dissolved organic matter. To directly observe carbon utilization by phytoplankton and identify potential CO₂ effects, tracers such as ¹³C provide much better insights (compare de Kluijver et al., 2010, 2012).

4.5 Temporal development of CO₂ effects

There are numerous standing stock or plankton assemblage composition parameters which were positively or negatively correlated with CO₂, sometimes even reversing from one to another phase. Interestingly, taking most of them together in a MDS and subsequent RELATE analysis shows that CO₂ related differences between mesocosms become increasingly significant with time (compare Table 3). For instance, although statistically not significant in phase I and II, significance levels of the RELATE analysis for the combined CHEMTAX and Chl *a* dataset steadily decreased from 0.425, 0.172 to 0.023 in phase I, II and III, respectively. Thus, it seems that CO₂ related differences slowly develop with time, becoming more and more pronounced and, consequently, statistically significant only after a certain period of time. The time necessary to detect such differences is probably connected to generation and turn-over times of the enclosed plankton communities and organic material. In this respect, the finding, that increasing temperatures (ranging between 2.5 and 8.5 °C) did not affect particulate maximum built-up of organic carbon and Chl *a* during a Baltic phytoplankton bloom in winter/spring (Wohlers et al., 2009) as opposed to a summer bloom (temperatures ranging between 9.5 to 17.5 °C) at the same location (Taucher et al., 2012), could be

Temporal biomass dynamics of an Arctic plankton bloom

K. G. Schulz et al.

Title Page

Abstract

Introduction

Conclusions

References

Tables

Figures



Back

Close

Full Screen / Esc

Printer-friendly Version

Interactive Discussion



connected to higher turn-over times at absolute higher temperatures and more rapidly evolving differences between treatments. Although, different temperature sensitivities of the dominating phytoplankton species in these two experiments cannot be ruled out (compare Taucher et al., 2012).

5 Finally, it seems that dissolved inorganic nutrients can be thought an amplifier. Upon addition, potential differences, for instance in phytoplankton community structure, too small to be detected at a statistically significant level, would be amplified during phytoplankton biomass built-up (as observed in this experiment during phase II). However, if added right after CO₂ manipulation, when differences between mesocosms are just starting to develop (as seen by the RELATE analysis), there is little to be amplified. 10 This could be the reason why a previous experiment could only detect statistically significant differences in phytoplankton community composition in the declining but not the built-up phase of a bloom (Schulz et al., 2008). Interestingly, it was then again the picoeukaryotes profiting from higher CO₂ levels, as observed in this experiment.

15 4.6 Dynamics in the fjord in comparison to the mesocosms

In the fjord, general temporal dynamics in many measured parameters such as particulate organic matter, Chl *a*, but also phytoplankton community structure (with some exceptions) was quite similar to those in the mesocosms, although occasionally at different absolute concentrations. For instance, Chl *a* also peaked in the fjord during phase I, declined and increased again in phase II, followed by a decline and an other increase in phase III, like in the mesocosms (compare Fig. 6a). This indicates that in the fjord at least similar processes, but most importantly triggers are at operation, although watermasses are constantly changing in comparison to the watermasses enclosed in the mesocosms. As light and temperature were identical inside and outside the meso- 20 cosms, both are potential triggers for observed biomass dynamics. Other shaping factors are the development of viral abundances and grazing on the plankton community, mainly responsible for autotrophic biomass decline. Different dissolved inorganic nutrient availability inside the mesocosms and the fjord, especially during phase II and III

Temporal biomass dynamics of an Arctic plankton bloom

K. G. Schulz et al.

Title Page

Abstract

Introduction

Conclusions

References

Tables

Figures



Back

Close

Full Screen / Esc

Printer-friendly Version

Interactive Discussion



rather seemed to determine absolute biomass than influence the temporal dynamics. In this respect, although maybe surprising, mesocosms appear capable to reflect natural processes and plankton succession at a certain location quite realistically, at least for a certain period of time.

5 *Acknowledgements.* This work is a contribution to the “European Project on Ocean Acidification” (EPOCA) which received funding from the European Community’s Seventh Framework Programme (FP7/2007–2013) under grant agreement no. 211384. Financial support was provided through Transnational Access funds by the European Union Seventh Framework Program (FP7/2007–2013) under grant agreement no. 22822 MESOAQUA and by Federal Ministry of Education and Research (BMBF, FKZ 03F0608) through the BIOACID (Biological Impacts of Ocean ACIDification) project. We gratefully acknowledge the logistical support of Greenpeace International for its assistance with the transport of the mesocosm facility from Kiel to Ny-Alesund and back to Kiel. We also thank the captains and crews of *M/V ESPERANZA* of Greenpeace and *R/V Viking Explorer* of the University Centre in Svalbard (UNIS) for assistance during mesocosm transport and during deployment and recovery in Kongsfjorden. We thank the staff of the French-German Arctic Research Base at Ny-Alesund, in particular Marcus Schumacher, for on-site logistical support. S. Koch-Klavsen acknowledges funding by “The Danish Council for Independent Research: Natural Sciences”.

20 The service charges for this open access publication have been covered by a Research Centre of the Helmholtz Association.

References

- 25 Aberle, N., Schulz, K. G., Stuhr, A., Ludwig, A., and Riebesell, U.: High tolerance of protozooplankton to ocean acidification in an Arctic coastal plankton community, *Biogeosciences Discuss.*, accepted, 2012. 12565, 12567
- Armstrong, R. A., Lee, C., Hedges, J. I., Honjo, S., and Wakeham, S.: A new, mechanistic model for organic carbon fluxes in the ocean based on the quantitative association of POC with ballast minerals, *Deep-Sea Res.*, 49, 219–236, 2001. 12566

Temporal biomass dynamics of an Arctic plankton bloom

K. G. Schulz et al.

Title Page

Abstract

Introduction

Conclusions

References

Tables

Figures



Back

Close

Full Screen / Esc

Printer-friendly Version

Interactive Discussion



Temporal biomass dynamics of an Arctic plankton bloom

K. G. Schulz et al.

[Title Page](#)[Abstract](#)[Introduction](#)[Conclusions](#)[References](#)[Tables](#)[Figures](#)[◀](#)[▶](#)[◀](#)[▶](#)[Back](#)[Close](#)[Full Screen / Esc](#)[Printer-friendly Version](#)[Interactive Discussion](#)

- Barlow, R. G., Cummings, D. G., and Gibb, S. W.: Improved resolution of mono- and divinyl chlorophylls a and b and zeaxanthin and lutein in phytoplankton extracts using reverse phase C-8 HPLC., *Mar. Ecol.-Prog. Ser.*, 161, 303–307, 1997. 12552
- 5 Bates, N. R., Mathis, J. T., and Cooper, L. W.: Ocean acidification and biologically induced seasonality of carbonate mineral saturation states in the Western Arctic Ocean, *J. Geophys. Res.*, 114, C11007, doi:10.1029/2008JC004862, 2009. 12546
- Bellerby, R. G. J., Silyakova, A., Nondal, G., Slagstad, D., Czerny, J., De Lange, T., and Ludwig, A.: Marine carbonate system evolution during the EPOCA Arctic pelagic ecosystem experiment in the context of simulated future Arctic ocean acidification, *Biogeosciences Discuss.*, accepted, 2012. 12550, 12563
- 10 Broecker, W. S. and Peng, T.-H.: *Tracers in the Sea*, Lamont-Doherty Earth Observatory, Palisades, NY, 1982. 12563
- Brussaard, C. P. D., Noordeloos, A. A. M., Witte, H., Collenteur, M. C. J., Schulz, K., Ludwig, A., and Riebesell, U.: Arctic microbial community dynamics influenced by elevated CO₂ levels, *Biogeosciences Discuss.*, in press, 2012. 12565, 12566, 12567
- 15 Clarke, K. R. and Warwick, R. M.: *Change in marine communities: an approach to statistical analysis and interpretations*, PRIMER-E Ltd., Plymouth, p. 144, 2001. 12554
- Clarke, K. R. and Gorley, R. N.: *Primer v6: user manual/tutorial*, PRIMER-E Ltd., Plymouth, p. 190, 2006. 12554
- 20 Clarke, K. R., Somerfield, P. J., Airoldi, L., and Warwick, R. M.: Exploring interactions by second-stage community analyses, *J. Exp. Mar. Biol. Ecol.*, 338, 179–192, 2006. 12553
- Cuvellier, M. L., Allen, A. E., Monier, A., McCrow, J. P., Messié, M., Tringe, S. G., Woyke, T., Welsh, R. M., Ishoey, T., Lee, J.-H., Binder, B. J., DuPont, C. L., Latasa, M., Guigand, C., Buck, K. R., Hilton, J., Thiagarajan, M., Caler, E., Read, B., Lasken, R. S., Chavez, F. P., and Worden, A. Z.: Targeted metagenomics and ecology of globally important uncultured eukaryotic phytoplankton, *P. Natl. Acad. Sci. USA*, 107, 14679–14684, 2010. 12567
- 25 Czerny, J., Bellerby, R. G. J., Boxhammer, T., Engel, A., Ludwig, A., Nachtigall, K., Niehoff, B., Nondal, G., Silyakova, A., Schulz, K. G., Sswat, M., and Riebesell, U.: Carbon budgets and fluxes in and Arctic mesocosm CO₂ perturbation study, *Biogeosciences Discuss.*, in preparation, 2012a. 12566, 12567
- 30 Czerny, J., Schulz, K. G., Krug, S., Ludwig, A., and Riebesell, U.: Volume estimate in mesocosms, *Biogeosciences Discuss.*, in preparation, 2012b. 12549

- de Kluijver, A., Soetaert, K., Schulz, K. G., Riebesell, U., Bellerby, R. G. J., and Middelburg, J. J.: Phytoplankton-bacteria coupling under elevated CO₂ levels: a stable isotope labelling study, *Biogeosciences*, 7, 3783–3797, doi:10.5194/bg-7-3783-2010, 2010. 12568
- de Kluijver, A., Soetaert, K., Czerny, J., Schulz, K. G., Boxhammer, T., Riebesell, U., and Middelburg, J. J.: A ¹³C labelling study on carbon fluxes in Arctic plankton communities under elevated CO₂ levels, *Biogeosciences Discuss.*, 9, 8571–8610, doi:10.5194/bgd-9-8571-2012, 2012. 12568
- Engel, A., Zondervan, I., Aerts, K., Beaufort, L., Benthien, A., Chou, L., Delille, B., Gattuso, J.-P., Harlay, J., Heemann, C., Hoffmann, L., Jacquet, S., Nejstgaard, J., Pizay, M. D., Rochelle-Newall, E., Schneider, U., Terbrueggen, A., and Riebesell, U.: Testing the direct effect of CO₂ concentration on a bloom of the coccolithophorid *Emiliania huxleyi* in mesocosm experiments, *Limnol. Oceanogr.*, 50, 493–507, 2005. 12568
- Engel, A., Schulz, K. G., Riebesell, U., Bellerby, R., Delille, B., and Schartau, M.: Effects of CO₂ on particle size distribution and phytoplankton abundance during a mesocosm bloom experiment (PeECE II), *Biogeosciences*, 5, 509–521, doi:10.5194/bg-5-509-2008, 2008. 12565
- Engel, A., Borchard, C., Piontek, J., Schulz, K., Riebesell, U., and Bellerby, R.: CO₂ increases ¹⁴C-primary production in an Arctic plankton community, *Biogeosciences Discuss.*, 9, 10285–10330, doi:10.5194/bgd-9-10285-2012, 2012. 12552
- Francois, R., Honjo, S., Krishfield, R., and Manganini, S.: Factors controlling the flux of organic carbon to the bathypelagic zone of the ocean, *Global Biogeochem. Cy.*, 16, 1087, doi:10.1029/2001GB001722, 2002. 12566
- Gattuso, J.-P., Lee, K., Rost, B., and Schulz, K. G.: Approaches and tools to manipulate the carbonate chemistry, in: *Guide to Best Practices in Ocean Acidification Research and Data Reporting*, edited by: Riebesell, U., Fabry, V. J., and Gattuso, J.-P., <http://www.epoca-project.eu/index.php/Home/Guide-to-OA-Research/>, 2010. 12550
- Giordano, M., Beardall, J., and Raven, J. A.: CO₂ concentrating mechanisms in algae: mechanisms, environmental modulation, and evolution, *Annu. Rev. Plant. Biol.*, 56, 99–131, 2005. 12566
- Hansen, H. P. and Koroleff, F.: Determination of nutrients, in: *Methods of Seawater Analysis*, edited by: Grasshoff, K. K. K. and Ehrhardt, M., John Wiley, Hoboken, NJ, 159–229, 1999. 12551, 12552

Temporal biomass dynamics of an Arctic plankton bloom

K. G. Schulz et al.

Title Page

Abstract

Introduction

Conclusions

References

Tables

Figures

◀

▶

◀

▶

Back

Close

Full Screen / Esc

Printer-friendly Version

Interactive Discussion



Temporal biomass dynamics of an Arctic plankton bloomK. G. Schulz et al.

[Title Page](#)[Abstract](#)[Introduction](#)[Conclusions](#)[References](#)[Tables](#)[Figures](#)[◀](#)[▶](#)[◀](#)[▶](#)[Back](#)[Close](#)[Full Screen / Esc](#)[Printer-friendly Version](#)[Interactive Discussion](#)

Holmes, R. M., Aminot, A., Kérgouel, R., Hooker, B. A., and Peterson, B. J.: A simple and precise method for measuring ammonium in marine and freshwater ecosystems, *Can. J. Fish. Aquat. Sci.*, 56, 1801–1808, 1999. 12551, 12552

Hop, H., Falk-Peterson, S., Svendsen, S., Kwasniewski, V., Pavlov, V., Pavlova, O., and Søreide, J. E.: Physical and biological characteristics of the pelagic system across Fram Strait to Kongsfjorden, *Progr. Oceanogr.*, 71, 182–231, 2006. 12564

Hoppenrath, M., Elbrächter, M., and Drebes, G. (Eds.): *Marine phytoplankton: selected microphytoplankton species from the North Sea around Helgoland and Sylt*, Schweizerbart Science Publishers, Stuttgart, 2009. 12553

Iglesias-Rodríguez, M. D., Nimer, N. A., and Merret, M. J.: Carbon dioxide-concentrating mechanism and the development of extracellular carbonic anhydrase in the marine picoeukaryote *Micromonas pusilla*, *New Phytol.*, 140, 685–690, 1998. 12566

Iversen, K. R. and Seuthe, L.: Seasonal microbial processes in a high-latitude fjord (Kongsfjorden, Svalbard): I. Heterotrophic bacteria, picoplankton and nanofagellates, *Polar. Biol.*, 34, 731–749, 2011. 12564

Kerouel, R. and Aminot, A.: Fluorometric determination of ammonia in sea and estuarine waters by direct segmented flow analysis, *Mar. Chem.*, 57, 265–275, 1997. 12553

Kim, J.-M., Lee, K., Shin, K., Yang, E. J., and Engel, A.: Shifts in biogenic carbon flow from particulate to dissolved forms under high carbon dioxide and warm ocean conditions, *Geophys. Res. Lett.*, 38, L08612, doi:10.1029/2011GL047346, 2011. 12568

Klaas, C. and Archer, D. E.: Association of sinking organic matter with various types of mineral ballast in the deep sea: implications for the rain ratio, *Global Biogeochem. Cy.*, 16, 1116, doi:10.1029/2001GB001765, 2002. 12566

Kraberg, A., Baumann, M., and Dürselen, C.-D.: *Coastal Phytoplankton: Photo Guide for Northern European Seas*, Pfeil, München, 2010. 12553

Kroeker, K. J., Kordas, R. L., Crim, R. N., and Singh, G. G.: Meta-analysis reveals negative yet variable effects of ocean acidification on marine organisms, *Ecol. Lett.*, 13, 1419–1343, 2010. 12546

Laws, E. A.: Photosynthetic quotients, new production and net community production in the open ocean, *Deep-Sea Res.*, 38, 143–167, 1991. 12563

Lui, H., Probert, I., Uitz, J., Claustre, H., Aris-Brosou, S., Frada, M., Not, F., and de Vargas, C.: Extreme diversity in noncalcifying haptophytes explains a major pigment paradox in open oceans, *P. Natl. Acad. Sci. USA*, 106, 10809–12808, 2009. 12567

Temporal biomass dynamics of an Arctic plankton bloomK. G. Schulz et al.

[Title Page](#)[Abstract](#)[Introduction](#)[Conclusions](#)[References](#)[Tables](#)[Figures](#)[◀](#)[▶](#)[◀](#)[▶](#)[Back](#)[Close](#)[Full Screen / Esc](#)[Printer-friendly Version](#)[Interactive Discussion](#)

Mackey, M. D., Mackey, D. J., Higgins, H. W., and Wright, S. W.: CHEMTAX – a program for estimating class abundances from chemical markers: application to HPLC measurements of phytoplankton, *Mar. Ecol.-Prog. Ser.*, 144, 265–283, 1996. 12552

Marinov, I., Doney, S. C., and Lima, I. D.: Response of ocean phytoplankton community structure to climate change over the 21st century: partitioning the effects of nutrients, temperature and light, *Biogeosciences*, 7, 3941–3959, doi:10.5194/bg-7-3941-2010, 2010. 12546

Meakin, N. G. and Wyman, M.: Rapid shifts in picoeukaryote community structure in response to ocean acidification, *ISME J.*, 5, 1397–1405, 2011. 12565

Mehrbach, C., Culberson, C. H., Hawley, J. E., and Pytkowicz, R. M.: Measurements of the apparent dissociation constants of carbonic acid in seawater at atmospheric pressure, *Limnol. Oceanogr.*, 18, 897–907, 1973. 12563

Menden-Deuer, S. and Lessard, E. L.: Carbon to volume relationships for dinoflagellates, diatoms, and other protist plankton, *Limnol. Oceanogr.*, 45, 569–579, 2000. 12553

Montagnes, D. J. S., Berges, A., Harrison, P. J., and Taylor, F. J. R.: Estimating carbon, nitrogen, protein, and chlorophyll *a* from volume in marine phytoplankton, *Limnol. Oceanogr.*, 39, 1044–1060, 1994. 12564, 12565

Newbold, L. K., Oliver, A. E., Booth, T., Tiwari, B., DeSantis, T., Maguire, M., Andersen, G., van der Gast, C., and Whiteley, A. S.: The response of marine picoplankton to ocean acidification, *Environ. Microbiol.*, 14, 2293–2307, doi:10.1111/j.1462-2920.2012.02762.x, 2012. 12565

Niehoff, B., Knüppel, N., Daase, M., Czerny, J., and Boxhammer, T.: Mesozooplankton community development at elevated CO₂ concentrations: results from a mesocosm experiment in an Arctic fjord, *Biogeosciences Discuss.*, 9, 11479–11515, doi:10.5194/bgd-9-11479-2012, 2012. 12565, 12567

Olenina, I., Hajdu, S., Edler, L., Andersson, A., Wasmund, N., Busch, S., Göbel, J., Gromisz, S., Huseby, S., Huttunen, M., Jaanus, A., Kokkonen, P., Ledaine, I., and Niemkiewicz: Biovolumes and size-classes of phytoplankton in the Baltic Sea, *HELCOM Balt. Sea Environ. Proc.*, 106, 1–144, 2006. 12553

Passow, U.: Switching perspectives: do mineral fluxes determine particulate organic carbon fluxes or vice versa?, *Geochem. Geophys. Geosy.*, 5, 1-5, ISSN 1525-2027, doi:10.1029/2003GC000670, 2004. 12566

- Sharp, J. H.: Improved analysis for 'particulate' organic carbon and nitrogen from seawater, *Limnol. Oceanogr.*, 19, 984–989, 1974. 12551
- Silyakova, A., Bellerby, R. G. J., Czerny, J., Schulz, K. G., Nondal, G., Tanaka, T., Engel, A., De Lange, T., and Riebesell, U.: Net community production and stoichiometry of nutrient consumption in a pelagic ecosystem of a northern high latitude fjord: mesocosm CO₂ perturbation study, *Biogeosciences Discuss.*, 9, 11705–11737, doi:10.5194/bgd-9-11705-2012, 2012. 12556
- Steinacher, M., Joos, F., Frölicher, T. L., Plattner, G.-K., and Doney, S. C.: Imminent ocean acidification in the Arctic projected with the NCAR global coupled carbon cycle-climate model, *Biogeosciences*, 6, 515–533, doi:10.5194/bg-6-515-2009, 2009. 12546
- Taucher, J., Schulz, K. G., Dittmar, T., Sommer, U., Oschlies, A., and Riebesell, U.: Enhanced carbon overconsumption in response to increasing temperatures during a mesocosm experiment, *Biogeosciences Discuss.*, 9, 3479–3514, doi:10.5194/bgd-9-3479-2012, 2012. 12568, 12569
- Tomas, C. R. (Ed.): Identifying marine phytoplankton, Academic Press, San Diego, 1997. 12553
- Uitz, J., Claustre, H., Gentili, B., and Stramski, D.: Phytoplankton class-specific primary production in the world's oceans: Seasonal and interannual variability from satellite observations, *Global Biogeochem. Cy.*, 24, GB3016, doi:10.1029/2009GB003680, 2010. 12567
- von Quillfeldt, C. H.: Ice algae and phytoplankton in north Norwegian and Arctic waters: species composition, succession and distribution, Ph.D. thesis, University of Tromsø, 1996. 12553
- Welschmeyer, N. A.: Fluorometric analysis of chlorophyll *a* in the presence of chlorophyll *b* and pheopigments, *Limnol. Oceanogr.*, 39, 1985–1992, 1994. 12552
- Wohlers, J., Engel, A., Zöllner, E., Breithaupt, P., Jürgens, K., Hoppe, H.-G., Sommer, U., and Riebesell, U.: Changes in biogenic carbon flow in response to sea surface warming, *P. Natl. Acad. Sci. USA*, 106, 7067–7072, 2009. 12568
- Worden, A. Z. Lee, J. H., Mock, T., Rouzé, P., Simmons, M. P., Aerts, A. L., Allen, A. E., Cuvellier, M. L., Derelle, E., Everett, M. V., Foulon, E., Grimwood, J., Gundlach, H., Hennissat, B., Napoli, C., McDonald, S. M., Parker, M. S., Rombauts, S., Salamov, A., Von Dassow, P., Badger, J. H., Coutinho, P. M., Demir, E., Dubchak, I., Gentemann, C., Eikrem, W., Gready, J. E., John, U., Lanier, W., Lindquist, E. A., Lucas, S., Mayer, K. F., Moreau, H., Not, F., Otilar, R., Panaud, O., Pangilinan, J., Paulsen, I., Piegu, B., Poliakov, A., Robbens, S., Schmutz, J., Toulza, E., Wyss, T., Zelensky, A., Zhou, K., Armbrust, E. V., Bhattacharya, D., Goode-nough, U. W., Van de Peer, Y., and Grigoriev, I. V.: Green evolution and dynamic adaptations

Temporal biomass dynamics of an Arctic plankton bloom

K. G. Schulz et al.

Title Page

Abstract

Introduction

Conclusions

References

Tables

Figures

◀

▶

◀

▶

Back

Close

Full Screen / Esc

Printer-friendly Version

Interactive Discussion



revealed by genomes of the marine picoeukaryotes *Micromonas*, *Science*, 324, 268–272, 2009. 12566

5 Yamamoto-Kawai, M., McLaughlin, F. A., Carmack, E. C., Nishino, S., and Shimada, K.: Aragonite undersaturation in the Arctic ocean: effects of ocean acidification and sea ice melt, *Science*, 326, 1098–1100, 2009. 12546

BGD

9, 12543–12592, 2012

Temporal biomass dynamics of an Arctic plankton bloom

K. G. Schulz et al.

Title Page

Abstract

Introduction

Conclusions

References

Tables

Figures

◀

▶

◀

▶

Back

Close

Full Screen / Esc

Printer-friendly Version

Interactive Discussion



Temporal biomass dynamics of an Arctic plankton bloom

K. G. Schulz et al.

Title Page

Abstract

Introduction

Conclusions

References

Tables

Figures

◀

▶

◀

▶

Back

Close

Full Screen / Esc

Printer-friendly Version

Interactive Discussion



Table 1. Amounts of CO₂ enriched seawater added to the mesocosms between day *t*−1 and day *t*4. Mesocosms which received no CO₂ addition got 25 l of 50 μm filtered natural seawater instead. Resulting pCO₂ (μatm) and pH (on the total scale) after equilibration with the deadspace are shown as a mean of day *t*8 and *t*9 values. Symbols and color code denote those used in Figs. 6, 7, 8, 9, 10 and 11.

	Fjord	M3	M7	M2	M4	M8	M1	M6	M5	M9
t-1				50 l	50 l	50 l	50 l	50 l	50 l	50 l
t0					25 l	75 l	75 l	75 l	75 l	75 l
t1						25 l	75 l	75 l	100 l	100 l
t2				20 l	20 l			30 l	40 l	75 l
t4						5 l	8 l		12 l	20 l
∑				70 l	95 l	155	208 l	230 l	277 l	320 l
pCO ₂		185	185	270	375	480	685	820	1050	1420
pH		8.32	8.31	8.18	8.05	7.96	7.81	7.74	7.64	7.51
	●	●	▲	■	●	▲	■	●	▲	■

Temporal biomass dynamics of an Arctic plankton bloom

K. G. Schulz et al.

Title Page

Abstract Introduction

Conclusions References

Tables Figures

◀ ▶

◀ ▶

Back Close

Full Screen / Esc

Printer-friendly Version

Interactive Discussion

Table 2. *F*, *p* and adjusted R^2 values of F-tests on linear regressions of all measurement parameters presented in Figs. 6, 7, 8, 9, 10 and 11 in each mesocosm and respective $p\text{CO}_2$ during the three experimental phases. Statistically significant correlations are marked in bold for positive and italic for negative $p\text{CO}_2$ correlations, respectively.

	adj. R^2	<i>F</i>	<i>p</i>	adj. R^2	<i>F</i>	<i>p</i>	adj. R^2	<i>F</i>	<i>p</i>	adj. R^2	<i>F</i>	<i>p</i>
	Chl <i>a</i>			ΔNO_3^-			HPLC			Microscopy		
phase I	-0.0264	0.79	0.402	-0.1173	0.16	0.701						
phase II	0.8301	40.08	< 0.001	0.8237	38.38	< 0.001						
phase III	<i>0.7487</i>	<i>24.83</i>	<i>0.002</i>	<i>0.6689</i>	<i>17.16</i>	<i>0.004</i>						
	POC			ΔPO_4^{3-}			Chl <i>a</i> HPLC			Total auto		
phase I	0.0450	1.38	0.279	-0.1087	0.22	0.656	-0.0344	0.73	0.420	0.0925	1.82	0.220
phase II	0.7813	29.58	0.001	0.7579	26.04	0.001	0.7471	24.64	0.002	0.7953	32.09	< 0.001
phase III	0.0004	1.00	0.350	<i>0.7554</i>	<i>25.71</i>	<i>0.001</i>	<i>0.491</i>	<i>8.72</i>	<i>0.021</i>	0.0785	1.68	0.236
	PON			NH_4^+			Chl <i>a</i> Prasinoc			OF auto		
phase I	-0.0167	0.87	0.324	-0.0874	0.36	0.569	0.4962	8.87	0.021	-0.0738	0.45	0.524
phase II	0.8342	42.25	< 0.001	<i>0.4903</i>	<i>8.69</i>	<i>0.021</i>	0.5534	10.91	0.013	0.0540	1.46	0.267
phase III	-0.1397	0.02	0.8939	0.4188	6.77	0.035	<i>0.3845</i>	<i>6.00</i>	<i>0.044</i>	0.3207	4.78	0.065
	POP			H_4SiO_4			Chl <i>a</i> Dino			Dino auto		
phase I	-0.0107	0.92	0.371	0.6325	14.77	<i>0.006</i>	-0.1008	0.27	0.621	0.3082	4.56	0.070
phase II	0.4886	8.64	0.022	<i>0.9016</i>	<i>74.32</i>	< 0.001	0.6092	13.48	0.008	0.7210	21.67	0.002
phase III	0.0216	1.18	0.314	0.1710	2.65	0.148	0.3797	5.90	0.046	0.1630	2.56	0.154
	DOC			POC/PON			Chl <i>a</i> Crypto			Crypto		
phase I	0.0967	1.86	0.215	-0.0270	0.79	0.404	0.8333	40.99	< 0.001	0.0135	1.11	0.327
phase II	0.7710	27.94	0.001	-0.1428	0.00	0.981	0.5622	11.27	0.012	0.6580	16.39	0.005
phase III	-0.1418	0.01	0.937	<i>0.5814</i>	<i>12.11</i>	<i>0.010</i>	0.3472	5.26	0.056	0.0449	1.38	0.279
	DON			POC/POP			Chl <i>a</i> Chloro			Chloro? Hapto?		
phase I	-0.0916	0.33	0.585	0.5695	11.58	0.011	-0.1332	0.06	0.814	0.0193	1.16	0.318
phase II	-0.1383	0.03	0.871	-0.0019	0.99	0.354	-0.1370	0.04	0.854	0.5640	11.35	0.012
phase III	-0.1301	0.08	0.789	0.0487	1.41	0.274	<i>0.4719</i>	<i>8.15</i>	<i>0.025</i>	0.2018	3.02	0.126
	DOP			PON/POP			Chl <i>a</i> Cyano					
phase I	-0.0762	0.43	0.531	0.4744	8.22	0.024	-0.1241	0.12	0.742			
phase II	-0.0100	0.92	0.369	0.0042	1.03	0.343	-0.1299	0.08	0.785			
phase III	0.0652	1.56	0.252	-0.1378	0.03	0.865	0.2029	3.04	0.125			
	BSi			DOC/DON			Chl <i>a</i> Diatom			Diatom		
phase I	-0.1267	0.10	0.760	-0.0730	0.46	0.521	-0.0849	0.37	0.560	NaN	NaN	NaN
phase II	0.8323	40.71	< 0.001	-0.1426	0.00	0.968	-0.1016	0.79	0.403	0.2015	1.77	0.226
phase III	-0.0986	0.28	0.612	-0.0860	0.37	0.564	0.2671	3.92	0.088	<i>0.5284</i>	<i>9.96</i>	<i>0.016</i>
	TSi			DOC/DOP			Chl <i>a</i> Chryso			Chryso		
phase I	<i>0.5093</i>	<i>9.30</i>	<i>0.019</i>	-0.1387	0.03	0.878	0.3960	6.25	0.041	-0.1427	0.00	0.973
phase II	<i>0.6432</i>	<i>15.42</i>	<i>0.006</i>	0.0699	1.60	0.246	0.4631	7.91	0.026	0.4487	7.51	0.029
phase III	0.1189	0.28	0.192	-0.0931	0.32	0.590	0.1735	2.68	0.146	0.1929	2.91	0.132
	BSi sediment			DON/DOP			Chl <i>a</i> Hapto			OF hetero		
phase I	-0.1048	0.24	0.638	-0.0248	0.81	0.399	-0.0233	0.82	0.396	-0.0738	0.45	0.524
phase II	0.4191	6.77	0.035	-0.1187	0.15	0.709	0.4891	8.66	0.021	0.0540	1.46	0.267
phase III	<i>0.6235</i>	<i>14.25</i>	<i>0.007</i>	0.1286	2.18	0.183	0.2632	3.86	0.090	0.3207	4.78	0.065



Temporal biomass dynamics of an Arctic plankton bloom

K. G. Schulz et al.

Table 3. Significance levels of the RELATE analyses for the CHEMTAX and Chl *a*, phytoplankton carbon biomass, and organics (POC, PON, POP, DON and DOP) datasets. While a dashed line indicates that there were too little observations for an analysis, bold numbers highlight a statistical significance below the 5 % level.

	CHEMTAX + Chl <i>a</i>	Phytoplankton	Organics
Phase 0	–	–	–
Phase I	0.425	–	0.943
Phase II	0.172	–	0.369
Phase III	0.023	–	0.11
Phase 0–III	0.001	0.048	0.222

Title Page

Abstract

Introduction

Conclusions

References

Tables

Figures

◀

▶

◀

▶

Back

Close

Full Screen / Esc

Printer-friendly Version

Interactive Discussion



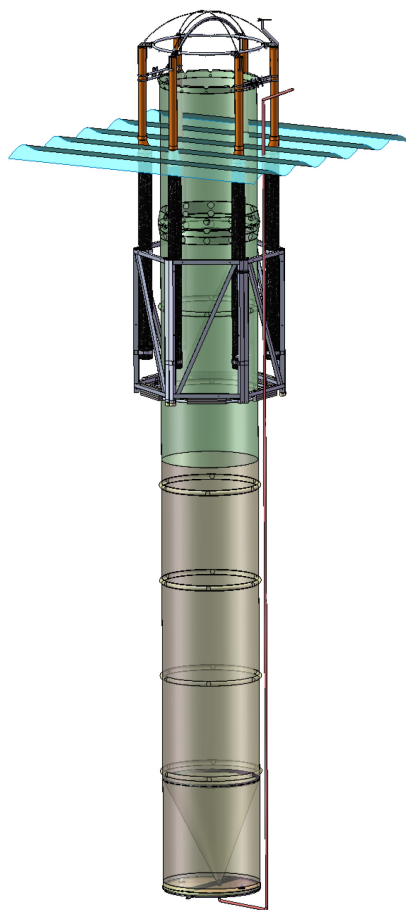


Fig. 1. Schematic drawing of a KOSMOS mesocosm deployed in the Kongsfjorden, with its characteristic deadspace below the sediment trap, shown in dark grey, at the bottom.

12581

BGD

9, 12543–12592, 2012

Temporal biomass dynamics of an Arctic plankton bloom

K. G. Schulz et al.

Title Page

Abstract

Introduction

Conclusions

References

Tables

Figures

◀

▶

◀

▶

Back

Close

Full Screen / Esc

Printer-friendly Version

Interactive Discussion



Temporal biomass dynamics of an Arctic plankton bloom

K. G. Schulz et al.

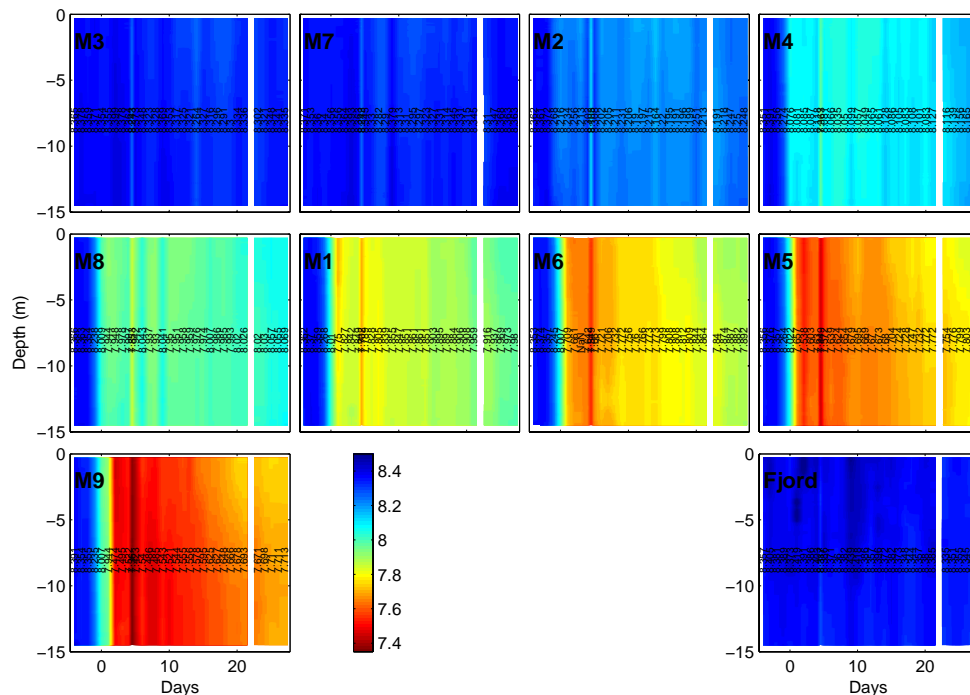


Fig. 3. Temporal dynamics of pH in each mesocosm and the fjord. Vertical profiles were taken daily by means of a hand-operated CTD. Recorded pH values were corrected by calculated pH from measured dissolved inorganic carbon and total alkalinity and are reported on the total scale. Black numbers denote daily depth-averaged (0.3–12 m) mean pH values. See Sect. 2 for further details.

Title Page

Abstract

Introduction

Conclusions

References

Tables

Figures

◀

▶

◀

▶

Back

Close

Full Screen / Esc

Printer-friendly Version

Interactive Discussion



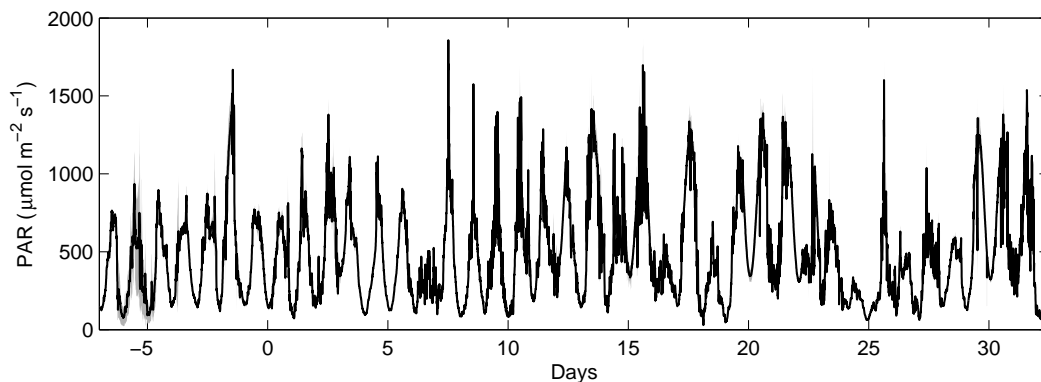


Fig. 4. Changes in photosynthetic active radiation (PAR) at ground level with time as measured by two LICOR sensors. The black line denotes the mean of both measurements while the grey shaded area illustrates the variability in between them.

Temporal biomass dynamics of an Arctic plankton bloom

K. G. Schulz et al.

Title Page

Abstract Introduction

Conclusions References

Tables Figures

◀ ▶

◀ ▶

Back Close

Full Screen / Esc

Printer-friendly Version

Interactive Discussion



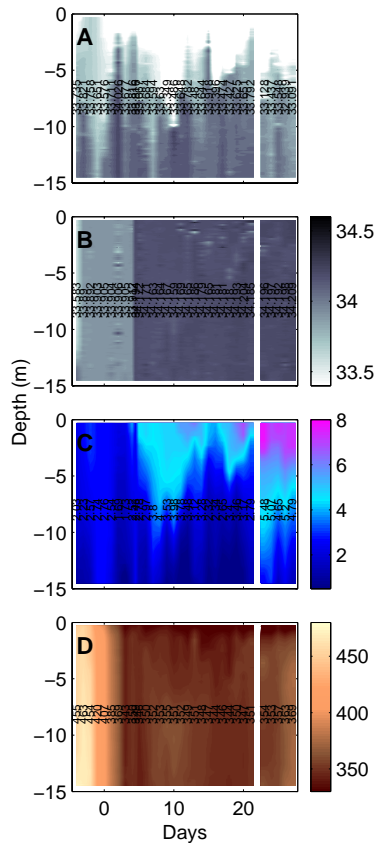


Fig. 5. Measured vertical distribution and change with time of salinity in the fjord (**A**) and mesocosm M1 (**B**), together with those of temperature (**C**) and oxygen concentration (**D**), reported in degrees Celsius and $\mu\text{mol kg}^{-1}$, respectively. Note that both vertical and temporal changes in salinity, temperature and oxygen were virtually identical between mesocosms. Vertical numbers denote depth-averaged (0.3–12 m) means of the respective parameter for each day.

Temporal biomass dynamics of an Arctic plankton bloom

K. G. Schulz et al.

Title Page

Abstract

Introduction

Conclusions

References

Tables

Figures

◀

▶

◀

▶

Back

Close

Full Screen / Esc

Printer-friendly Version

Interactive Discussion

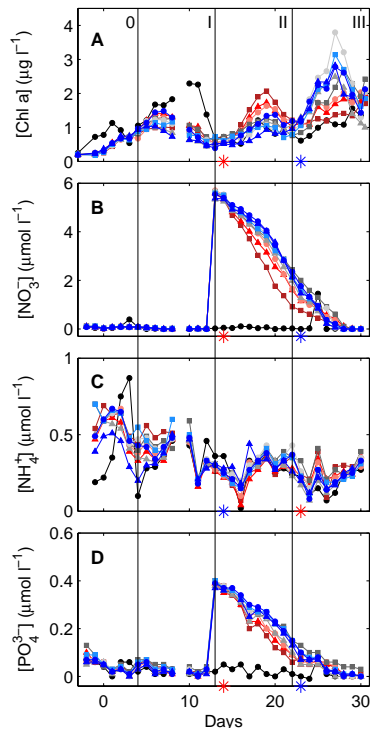


Fig. 6. Temporal development of depth-averaged (0.3–12 m) Chl *a* (**A**), nitrate (**B**), ammonium (**C**) and phosphate (**D**) concentrations in each mesocosm and the fjord. For symbols and color code see Table 1. Vertical black lines and Roman numbers illustrate the three phases after CO₂ perturbation while 0 refers to the phase prior to this event. Red and blue stars denote statistically significant positive and negative correlations during a certain phase, respectively. For details on and results of the statistics applied see Sect. 2.7 and Table 2. Note that statistics for nitrate and phosphate was done on rates not the actual concentrations.

Temporal biomass dynamics of an Arctic plankton bloom

K. G. Schulz et al.

Title Page

Abstract

Introduction

Conclusions

References

Tables

Figures

◀

▶

◀

▶

Back

Close

Full Screen / Esc

Printer-friendly Version

Interactive Discussion



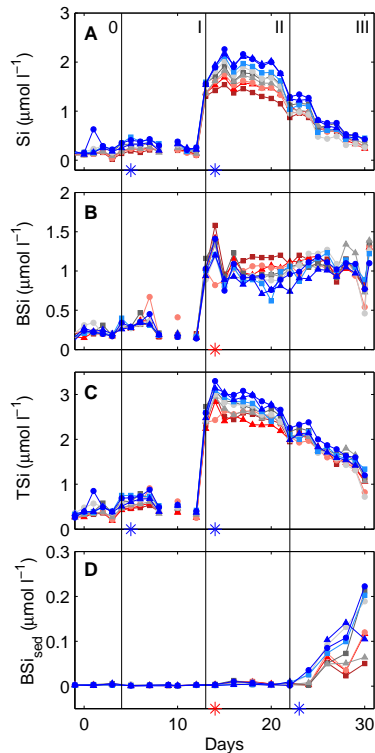


Fig. 7. Temporal development of depth-averaged (0.3–12 m) silicate **(A)**, biogenic silicate **(B)**, total silicate as the sum of silicate and biogenic silicate **(C)** and sedimented biogenic silicate concentrations **(D)**. Style and color code follow those of Fig. 6 and statistical results are summarized in Table 2.

Temporal biomass dynamics of an Arctic plankton bloom

K. G. Schulz et al.

Title Page

Abstract

Introduction

Conclusions

References

Tables

Figures

◀

▶

◀

▶

Back

Close

Full Screen / Esc

Printer-friendly Version

Interactive Discussion



Temporal biomass dynamics of an Arctic plankton bloom

K. G. Schulz et al.

Title Page

Abstract

Introduction

Conclusions

References

Tables

Figures

◀

▶

◀

▶

Back

Close

Full Screen / Esc

Printer-friendly Version

Interactive Discussion

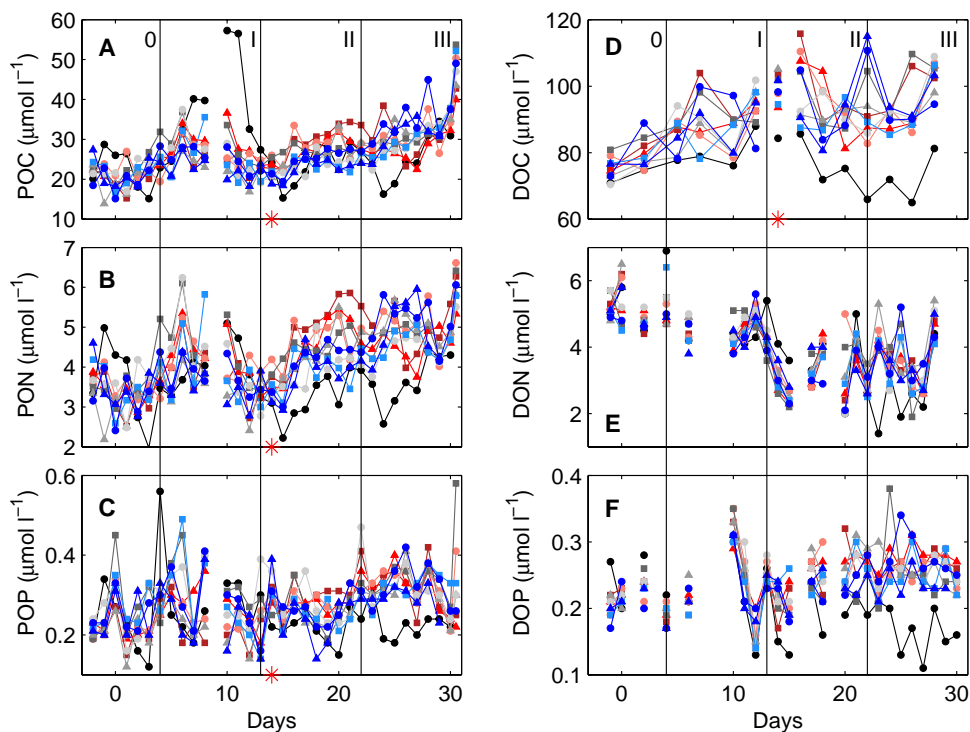


Fig. 8. Temporal development of depth-averaged (0.3–12 m) particulate organic carbon (A), nitrogen (B) and phosphorus (C), together with dissolved organic carbon (D), nitrogen (E) and phosphorus (F) concentrations. Style and color code follow those of Fig. 6 and statistical results are summarized in Table 2.

Temporal biomass dynamics of an Arctic plankton bloom

K. G. Schulz et al.

Title Page

Abstract

Introduction

Conclusions

References

Tables

Figures

◀

▶

◀

▶

Back

Close

Full Screen / Esc

Printer-friendly Version

Interactive Discussion

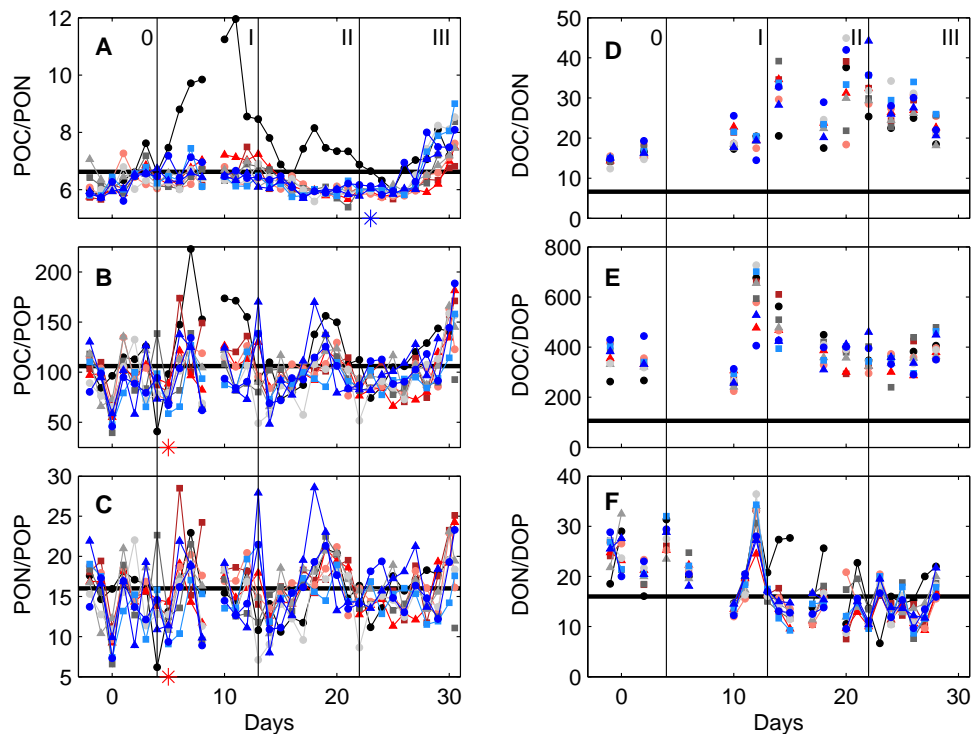


Fig. 9. Temporal development of depth-averaged (0.3–12 m) ratios of particulate organic carbon to nitrogen (**A**), particulate organic carbon to phosphorus (**B**), particulate organic nitrogen to phosphorus (**C**), dissolved organic carbon to nitrogen (**D**), dissolved organic carbon to phosphorus (**E**), and dissolved organic nitrogen to phosphorus (**F**). Horizontal black lines denote elemental ratios according to Redfield et al. (1963). Style and color code follow those of Fig. 6 and statistical results are summarized in Table 2.

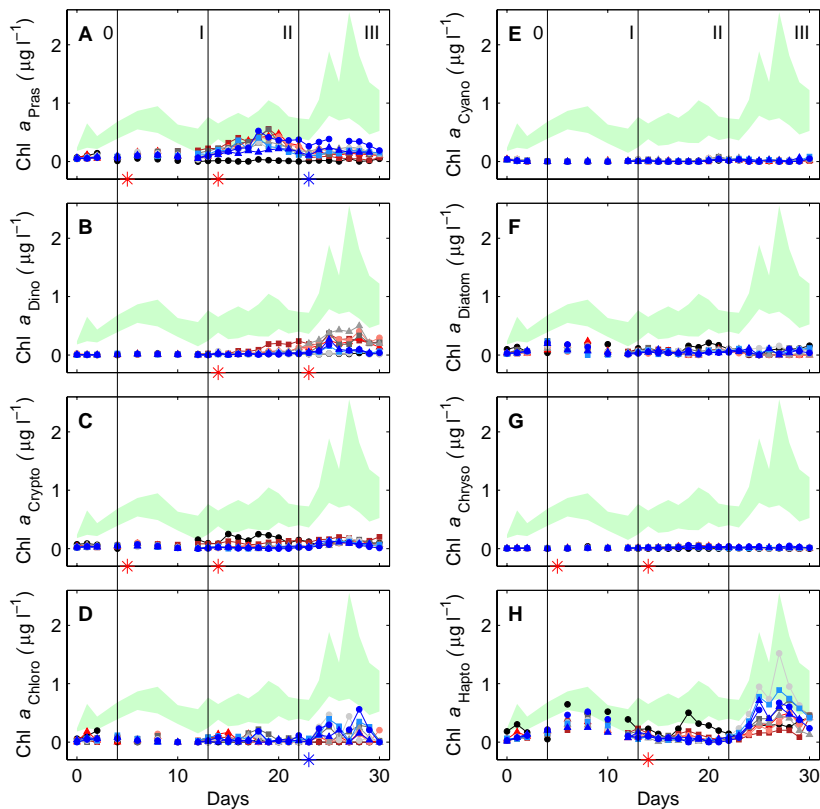


Fig. 10. Temporal development of depth-averaged (0.3–12 m) Chl *a* equivalent concentrations of prasinophytes (A), dinoflagellates (B), cryptophytes (C), chlorophytes (D), cyanobacteria (E), diatoms (F), chrysophytes (G) and haptophytes (H) as analyzed by HPLC and CHEMTAX (see Materials and Methods section for details). Green shaded area illustrates minima and maxima of total Chl *a* concentrations in the mesocosms. Style and color code follow those of Fig. 6 and statistical results are summarized in Table 2.

Temporal biomass dynamics of an Arctic plankton bloom

K. G. Schulz et al.

Title Page

Abstract

Introduction

Conclusions

References

Tables

Figures

◀

▶

◀

▶

Back

Close

Full Screen / Esc

Printer-friendly Version

Interactive Discussion



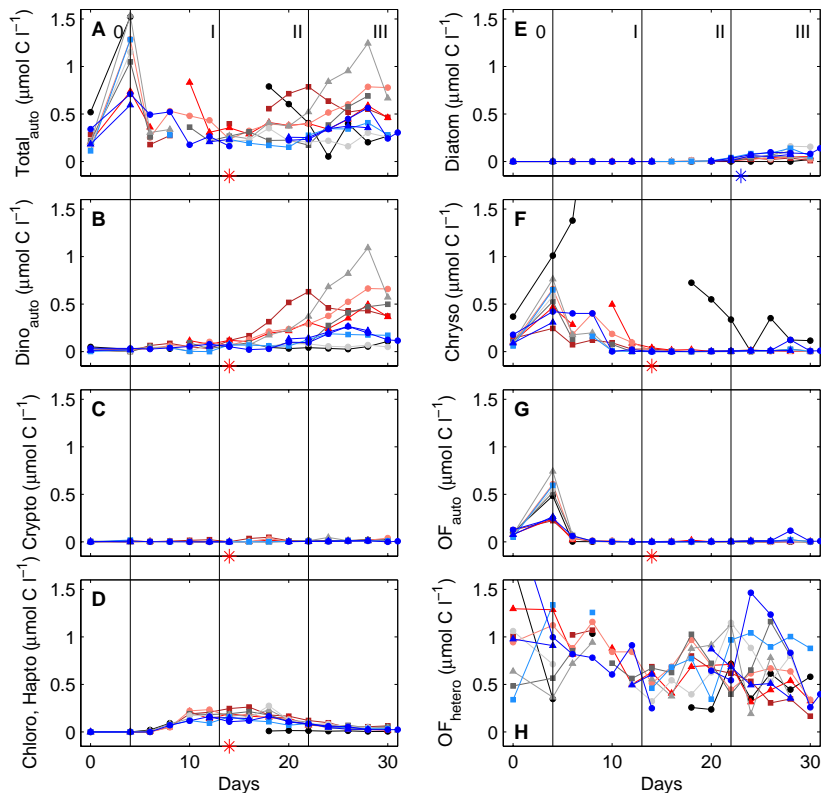


Fig. 11. Temporal development of depth-averaged (0.3–12 m) plankton carbon biomass of all autotrophs **(A)**, autotrophic dinoflagellates **(B)**, cryptophytes **(C)**, chloro- or haptophytes **(D)**, diatoms **(E)**, chrysophytes **(F)**, autotrophic flagellates other than dinoflagellates **(G)**, and heterotrophic flagellates **(H)** as counted by light microscopy. Style and color code follow those of Fig. 6 and statistical results are summarized in Table 2.

Temporal biomass dynamics of an Arctic plankton bloom

K. G. Schulz et al.

Title Page

Abstract Introduction

Conclusions References

Tables Figures

◀ ▶

◀ ▶

Back Close

Full Screen / Esc

Printer-friendly Version

Interactive Discussion



Temporal biomass dynamics of an Arctic plankton bloom

K. G. Schulz et al.

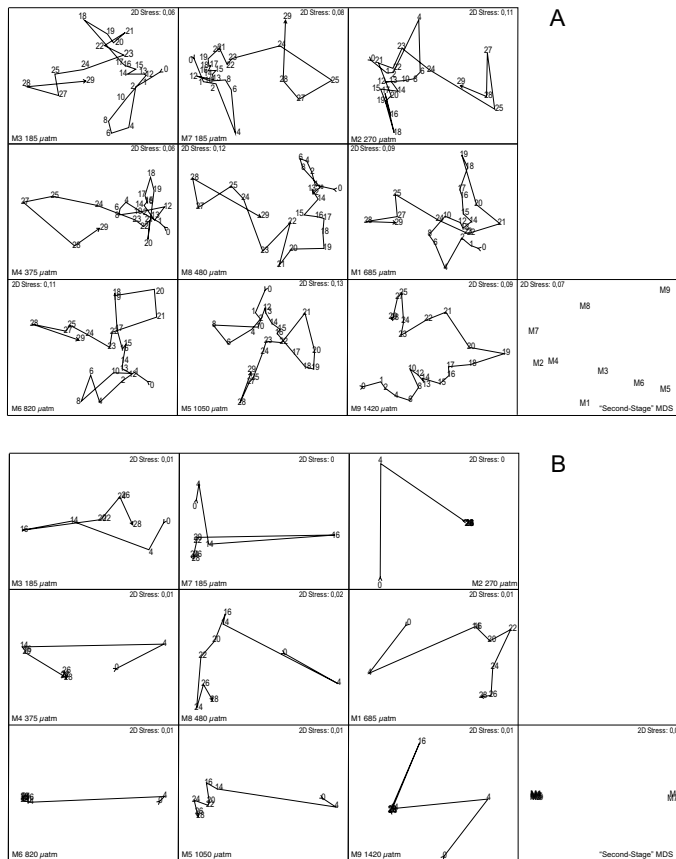


Fig. 12. First-stage MDS time trajectories and second-stage MDS plots from analyses of the CHEMTAX together with Chl *a* (**A**), and phytoplankton carbon biomass datasets (**B**). See Sect. 2.7.2 for details.